

A review on additive/subtractive hybrid manufacturing of directed energy deposition (DED) process



Mohammadreza Lalegani Dezaki^a, Ahmad Serjouei^a, Ali Zolfagharian^b, Mohammad Fotouhi^c, Mahmoud Moradi^d, M.K.A. Ariffin^e, Mahdi Bodaghi^{a,*}

^a Department of Engineering, School of Science and Technology, Nottingham Trent University, Nottingham, NG11 8NS, UK

^b School of Engineering, Deakin University, Geelong, 3216, Australia

^c Department of Materials, Mechanics, Management and Design (3MD), Delft University of Technology, Delft, the Netherlands

^d School of Mechanical, Aerospace and Automotive Engineering, Faculty of Engineering, Environment and Computing, Coventry University, Coventry, CV1 2JH, UK

^e Department of Mechanical and Manufacturing Engineering, Faculty of Engineering, Universiti Putra Malaysia, Serdang, 43400, Malaysia

ARTICLE INFO

Keywords:

Additive manufacturing
Additive/subtractive hybrid manufacturing
3D printing
Hybrid manufacturing
Metal alloys
Direct energy deposition
Machining

ABSTRACT

Additive manufacturing (AM) processes are reliable techniques to build highly complex metallic parts. Direct energy deposition (DED) is one of the most common technologies to 3D print metal alloys. Despite a wide range of literature that has discussed the ability of DED in metal printing, weak binding, poor accuracy, and rough surface still exist in final products. Thus, limitations in 3D printing of metal powder and wire indicate post-processing techniques required to achieve high quality in both mechanical properties and surface quality. Therefore, hybrid manufacturing (HM), specifically additive/subtractive hybrid manufacturing (ASHM) of DED has been proposed to enhance product quality. ASHM is a capable process that combines two technologies with 3-axis or multi-axis machines. Different methods have been suggested to increase the accuracy of machines to find better quality and microstructure. In contrast, drawbacks in ASHM still exist such as limitations in existing reliable materials and poor accuracy in machine coordination to avoid collision in the multi-axes machine. It should be noted that there is no review work with focuses on both DED and hybridization of DED processes. Thus, in this review work, a unique study of DED in comparison to ASHM as well as novel techniques are discussed with the objective of showing the capabilities of each process and the benefits of using them for different applications. Finally, new gaps are discussed in ASHM to enhance the layer bonding and surface quality with the processes' effects on microstructures and performance.

1. Introduction

Over the past few decades, a wide range of conventional technologies have been applied to producing metallic components in different industrial sectors. These processes are known as subtractive technology, transformative processes, and dividing operations which have specific features and characteristics in producing various end-use products. In spite of their capabilities in manufacturing sectors, inherent drawbacks due to the technological limitations exist accordingly [1]. For example, material waste, high cost, time-consuming process, and limitations in producing complex samples with sharp corners and thin walls are the main drawbacks that need to be eliminated in conventional processes [2]. Therefore, researchers have developed a novel technology which is called rapid prototyping (RP), or additive manufacturing (AM). 3D

printing, direct digital manufacturing (DDM), layered manufacturing (LM), and additive fabrication are encircled as the subsets of AM [3]. In contrast to conventional processes, AM follows the opposite direction in building products. It builds the products from the bottom to the top by fusing and binding materials layer by layer. Also, this technology can remove traditional processes' limitations due to its features in producing complex products. A vast range of materials from metals, thermoplastics, ceramics, and composites can be used in this technology based on machine characteristics [4,5].

As shown in Fig. 1, AM is categorized into seven processes commonly used to build a product due to high accuracy, repeatability, and precision [6]. Despite the same nature and characteristics of AM processes, each of them has specific features and is useful to print materials in form of solid, liquid, and powder [7,8]. Using this technology in industries helps manufacturers to produce customized products without assembling [9].

* Corresponding author.

E-mail address: mahdi.bodaghi@ntu.ac.uk (M. Bodaghi).

<https://doi.org/10.1016/j.apmate.2022.100054>

Received 18 December 2021; Received in revised form 9 April 2022; Accepted 11 April 2022

Available online 16 April 2022

2772-834X/© 2022 Central South University. Publishing services by Elsevier B.V. on behalf of KeAi Communications Co. Ltd. This is an open access article under the CC BY-NC-ND license (<http://creativecommons.org/licenses/by-nc-nd/4.0/>).

List of abbreviation

AM	additive manufacturing	KAM	kernel average misorientation
ASHM	additive/subtractive hybrid manufacturing	LDMD	laser direct metal deposition
ArchLM	arc hybrid layer manufacturing	LPD	layer powder deposition
CAD	computer aided design	LMD	laser metal deposition
CNC	computer numerical control	LWWAM	laser wire welding additive manufacturing
CMT	cold metal transfer	LM	layered manufacturing
DDM	direct digital manufacturing	MAG	metal active gas
DMD	direct metal deposition	PAW	plasma arc welding
DFM	design for manufacturing	RP	rapid prototyping
FEA	finite element analysis	RLWDED	robotized laser/wire directed energy deposition
FDM	fused deposition modelling	SEM	scanning electron microscope
FGM	functionally graded materials	SM	subtractive manufacturing
GMAW	gas metal arc welding	STL	standard tessellation language
GTAW	gas tungsten arc welding	S/N	signal-to-noise
HM	hybrid manufacturing	SR	surface roughness
HIP	hot isostatic pressing	TO	topology optimization
HAM	hybrid additive manufacturing	TIG	tungsten inert gas
		UTS	ultimate tensile strength
		WAAM	wire arc additive manufacturing

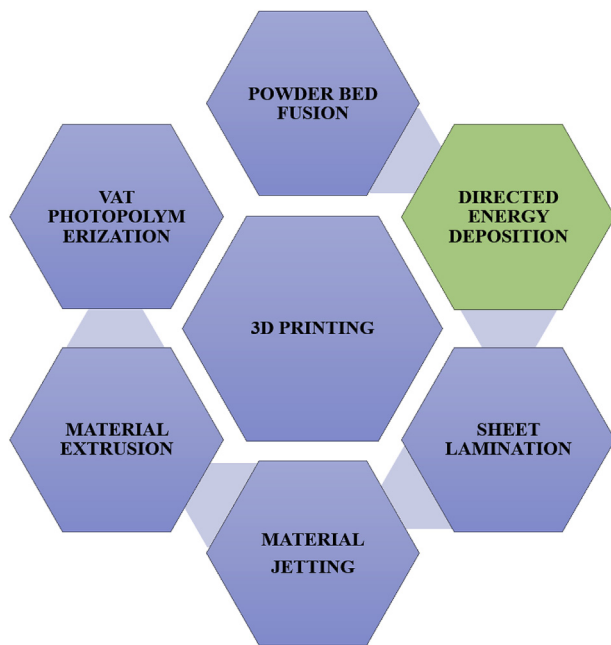


Fig. 1. Additive manufacturing processes.

Thus, the number of components is decreased and the final product is lighter and cheaper [10]. In AM technologies, the first step is to design part in computer-aided design (CAD) software. The following step is to convert the CAD design into a readable format which is known as standard tessellation language (STL) format. Exclusive software packages are available in the market which are able to slice and convert the CAD file into readable format. The 3D printer machine follows the path to print the parts layer by layer from the bottom to the top. This procedure is repeated constantly to finish the products. Different parameters are effective and have an extraordinary impact on the final quality and mechanical properties. Building orientation, layer thickness, temperature, material properties, nozzle diameter, scan speed, and laser power are the common factors in AM processes [11]. Hence, before printing, identifying proper parameters, part geometry decomposition, and process sequence to finish printing are the keys to maximizing the quality.

Metal alloys have been used in different applications due to their good properties and reliable characteristics [12]. Metal printing systems are divided into three categories, namely, powder bed systems, powder feed systems, and wire feed systems [13]. Directed energy deposition (DED) is one of the most common methods in printing metal alloys. DED processes are improving day by day and building novel metallic components is easier and faster in different fields. This technology is capable of printing different products with good accuracy, quality, and uniformity of materials. The ability to print highly complex features with different sizes is the key in DED process [14]. Many types of research have been conducted to increase the efficiency and productivity of these technologies [15]. In this technology, the laser source is the vital element to fuse powder by following the generated G-codes from exclusive software. Rapid solidification, directional cooling, and phase transformations are the main elements that affect the metal microstructures in DED process. However, a limited range of metal alloys is available in form of powder or wire shape for 3D printing [16].

Despite powerful DED processes to build different products, issues related to surface texture and mechanical properties still exist. DED uses a support structure to print objects based on required conditions to have better adhesion and accuracy [17]. Supports stiffen the printed layers in perpendicular angles and prevent material drops and distortions. Therefore, this structure is vital in this technology, but drawbacks should be eliminated as well. The quality of areas where the machine uses supports is not as good as other sections. Thus, to improve the surface quality, post-processing techniques are needed. Post-processing technologies are categorized into subtractive techniques, heat treatment, and chemical reactions when high precision is required [18]. Meanwhile, the procedure of printing and post-processing is time-consuming, and significant effort is needed to achieve the highest quality.

One of the best ways to eliminate limitations in these technologies is to combine DED and subtractive processes. A combination of AM and subtractive processes within the same machine is known as hybrid manufacturing (HM). HM can eliminate the relevant issues in both AM and machining in producing metallic components due to its features and capabilities. However, this process is still in its infancy and extensive research works are required to improve and optimize its features. The stability of each manufacturing process is important. Thus, point of tool initiation, machine calibration, and proper printing conditions are vital as well. Limitations in microstructure, poor binding and accuracy in the machine, and materials are the main concerns in additive/subtractive hybrid manufacturing (ASHM). This integration is a surpassing advanced technology to build products faster. High flexibility, less cost, part

reliability, and saving material are the main advantages of ASHM over DED process.

Literature works are focused on both subtractive, AM processes, and manufacturing process chains to elaborate their influence on production cost and time [19]. Besides, the supporting structure needed in AM process can be eliminated by ASHM due to more freedom and wider path planning. The ability of customized setup angles, tools depth, and tool containment boundaries of each surface is calculated to minimize the defects accordingly. However, extensive human effort is needed for subtractive processes, and ASHM is designed properly to reduce human interaction. Many researchers covered DED parameters and their features to illustrate how post-processing is needed in specific cases [20]. However, the impact of electric power and machine tooling should be determined.

Numerous review papers investigated both DED and ASHM separately while there is no comprehensive review considering both DED and ASHM simultaneously. This work provides insights on the differences between DED and ASHM in terms of microstructure features, cost effectiveness, process parameters, and technologies. Discussing the key features of these two processes and their impacts on the quality and showing how they are different in terms of process capabilities are the main elements of this work. Besides, a few works show the gaps and limitations in DED, while this study elaborates the role of ASHM in eliminating DED defects. Hence, the use of subtractive processes needs to be discussed to find out their effect on final printed products. The uniqueness of this study is to investigate how DED and ASHM processes manufacture products in detail with a wide range of discussion on microstructure and surface texture. Then, ASHM processes are discussed to show how these processes vary in terms of producing metal components. The obtained results provide details for researchers and industries to understand how DED and ASHM of the DED process work and the benefits of ASHM over DED. The first section focuses on an overall review of DED processes and their branches. Then, a more detailed discussion review about the DED process and its capabilities is presented. Issues in DED metal printing are discussed to show a better perspective of HM's role in industries. The following sections cover the DED hybridization and research works on their developments and strategies. Then, there is a comparison between DED and ASHM and the final section covers challenges and gaps in these technologies that require further research works.

2. Directed energy deposition (DED) processes

2.1. Basics of the process

DED process, which is known as 3D welding, can produce near net shape samples from powder or wire by laser energy source [21]. The basic schematic of the DED process is shown in Fig. 2. This technology can repair damages or build a new metal part like nickel alloys [22]. DED covers a vast range of applications such as aerospace (blade, engine components, and brackets), medical (implants, scaffolds, and earplug), and automotive (gear, knob, gearbox, and bumpers) due to its capability to produce metal parts by reducing assembly components. Focused thermal energy sources are laser, plasma arc, and electron beam that can melt or fuse the material [23]. The material is formed and deposited layer by layer from the bottom to the top. The key points to use in the DED process are repairing components, printing complex metallic products, and cladding in coating applications. Commonly, the printed products with DED exhibit poorer ductility and higher strength at constant parameters compared to the conventional methods for titanium alloys [24]. However, various elements from laser to nozzle torch and geometry should be considered to achieve reasonable results [25].

Process parameters are important in DED due to their role in producing metallic parts with different mechanical properties. To melt and micro-weld different wires, the laser energy must be high enough to melt powder properly [26]. Unlike SLM, the support material is not commonly used in this technology, but based on the product's geometry, support may be used to have better stability in printing products. The common materials

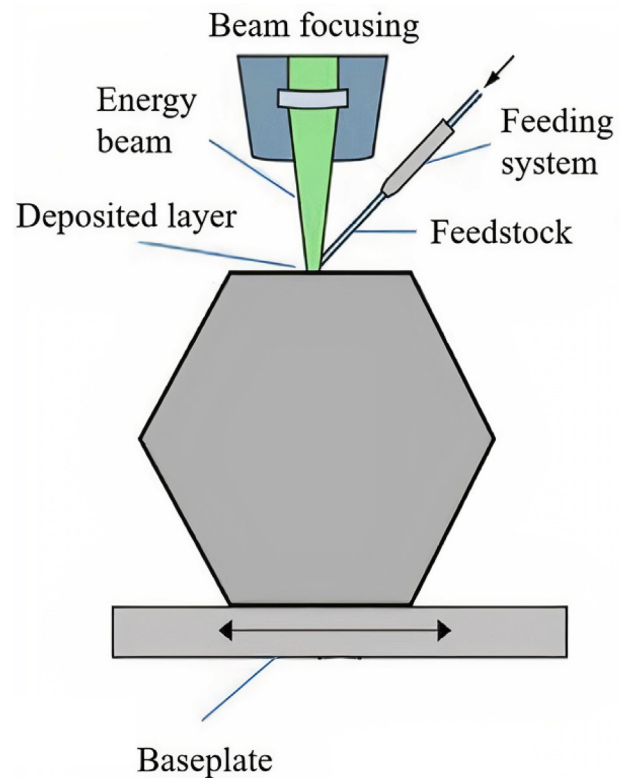


Fig. 2. Schematic of basic DED process.

are metal alloys with a wide range of properties in form of powder-like titanium, copper, gold, aluminum, and iron. Many factors play a role in increasing the quality and affect the mechanical properties, but laser power, laser scanning, and spot diameter are the important ones. For example, increasing the laser power helps to decrease the material deposition time and full melting occurs to achieve fully dense part without any post-process densification. Meanwhile, by decreasing the spot diameter, high energy densities in melted metal lead to better adhesion and the porosity decreases accordingly. In addition, surface roughness (SR) and direction of the elongated grains of printed parts have a positive correlation with laser power and scan speed. Also, the laser energy transfer becomes shorter if the scan speed increases. Thus, failure of melt spreading occurs when the laser energy is insufficient. This means that porosity and tendency increase which is caused by high cooling rates in response to high scan speeds. Also, mechanical stability and good heating dissipation depend on the substrate plate and nozzle torch. Highly graded and functionalized components can be easily produced due to the existence of powder form material. On the other hand, easy to use and store, high deposition rates, and high efficiency are the main advantages of wire form materials in the DED process. In brief, the nature of defects, formation of intermetallic strengthening phases, undesirable phases, the evolution of microstructure, and thus the mechanical properties are affected by scan speed and laser power.

Inherent rapid heating and cooling rate in DED process allow researchers to build superior quality parts. Flow rate, machine feed rate, and laser power are the critical parameters that affect the surface quality and mechanical properties to build complex geometric products [27]. The powder feed in DED is either by gravity or pneumatically in an inert gas stream. In some cases, due to the poor printing, the remaining unfused powder in powder-based DED brings many problems such as cost and material contamination [28]. Also, titanium and aluminum alloys are classified as highly reactive powders with fire risk. Meanwhile, reusing the waste powder is difficult and not efficient in powder-based processes. Instead of powder material, another alternative way is to print samples from metal wire.

DED is divided into different processes based on their features and characteristics (see Fig. 3). These differences are divided into the material, laser power, powder delivery, inert gas delivery, and path planning control. Various names have been assigned to these processes while the features and printing are the same. The laser is the key to solidifying and melting the material in the printing process. The value of 0.3–1 mm is the range of layer thickness in common DED processes, while using micro-laser in DED, it can be around 700–800 μm. Material deposition and part quality are affected by thermal behavior in this technology. A small zone is affected by high laser energy density and solidifies quickly. This procedure makes repeatability difficult due to its impact on part geometry [29]. Poor repeatability occurs when the process parameters are not optimized. As an example, insufficient laser power or high scan speed guide to unmelt the wire or powder accordingly. Hence, the melted layer is poor and solidified imperfectly. Meanwhile, as soon as the machine melts the next layer, it cannot attach to the previous one. Thus, poor adhesion and bonding occur between the layers and adversely affect the 3D printer repeatability.

2.2. Wire-feed additive manufacturing processes

Wire-feed technologies are used to produce large and moderate complex structures such as flanges. This system is categorized into laser wire welding additive manufacturing (LWWAM) and wire arc additive manufacturing (WAAM). LWWAM uses laser as the main energy source and wire metal to build metal products. The metal wire can be cold or hot based on requirements [30]. The main components of this process are a laser, automatic wire-feed system, preheating or cooling system, and hot or cold metal wire (see Fig. 4). The advantage of using hot wire instead of cold wire is saving more laser energy [31]. This method is similar to the common DED process but the main energy source is the laser. The motion system consists of a welding torch that melts the solid material which is fed into the melting pool. A wide range of spool alloys is available in the market based on requirements. In this technique, laser power is vital to achieving high quality.

Arc-based DED is known as ‘wire + arc’ additive manufacturing (WAAM) and the material is in form of wire which is like the filament in the fused deposition modelling (FDM) process [32]. As shown in Fig. 5(a) and (b), and (c), the WAAM process is categorized into three different processes, namely, gas metal arc welding (GMAW)-based [33], gas tungsten arc welding (GTAW)-based [34], and plasma arc welding (PAW)-based [35]. The material deposition time of GTAW or PAW is two times shorter than that of the GMAW process, while due to the electric current acting on the feedstock, this process is not as stable as GTAW and PAW. The mentioned techniques are based on co-axial and off-axis feeding. The main disadvantages of these processes are low

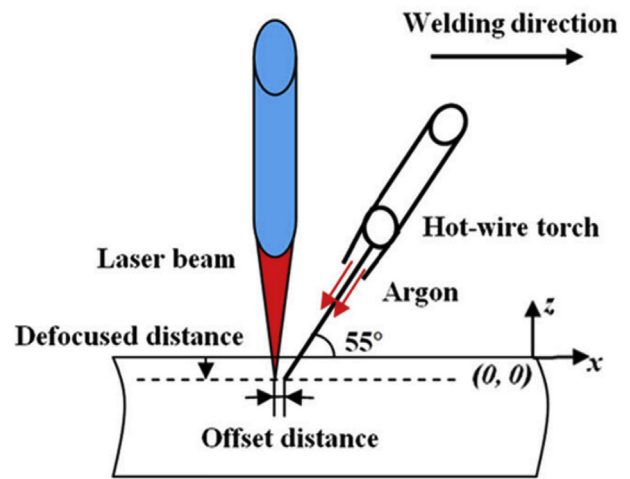


Fig. 4. Schematic of LWWAM process [30].

repeatability, poor adaptive control, accumulative error, and expensive post-processing technologies. Better surface quality, material deposition, and lower cost compared to the laser and electron beam melting are the main advantages of wire-feed DED processes [36]. These processes are capable of eliminating limitations such as low deposition rates and part size in the PBF process. Also, 15%–20% of the post-machining time is reduced by using WAAM compared to the traditional manufacturing processes [37]. These processes provide opportunities for the manufacturer in different fields to produce high-quality products. Titanium alloys, aluminum alloys, steel, nickel-based superalloys, and other metal alloys are the most important materials in these processes. Despite the capabilities that WAAM brings in industries, issues and defects such as porosity, delamination, and oxidation still exist in this method. Meanwhile, post-processing techniques are alternative ways to reduce limitations. Heat treatment, work hardening, and interpass gas cooling are required as secondary processes to enhance final products.

2.3. Laser direct metal deposition (LDMD)

Another process of DED is laser direct metal deposition (LDMD) by which metal powder is used to fabricate a wide range of products [39]. The schematic of the process is shown in Fig. 6. This process is suitable for the aerospace industry due to its high level of accuracy and precision [40]. Metal powder is injected directly following laser irradiation to build 3D CAD file layer by layer. Similar to other DED processes, process variables such as laser power and material flow are important to enhance the

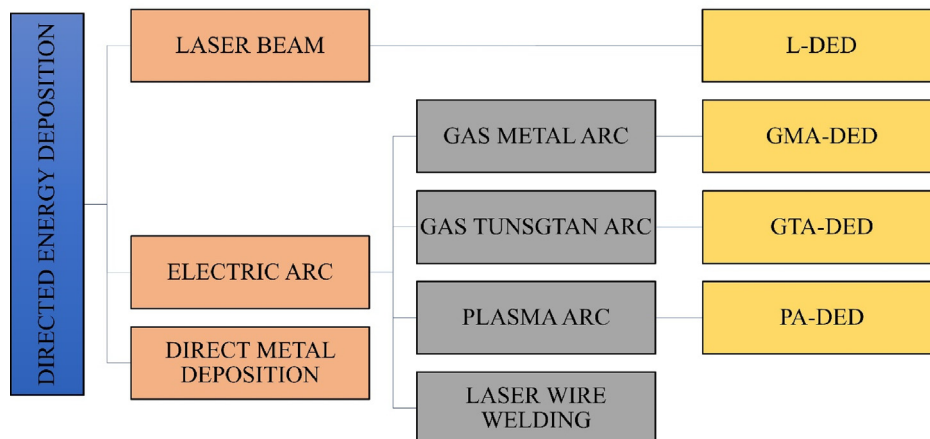


Fig. 3. Classification of DED process in 3D metal printing.

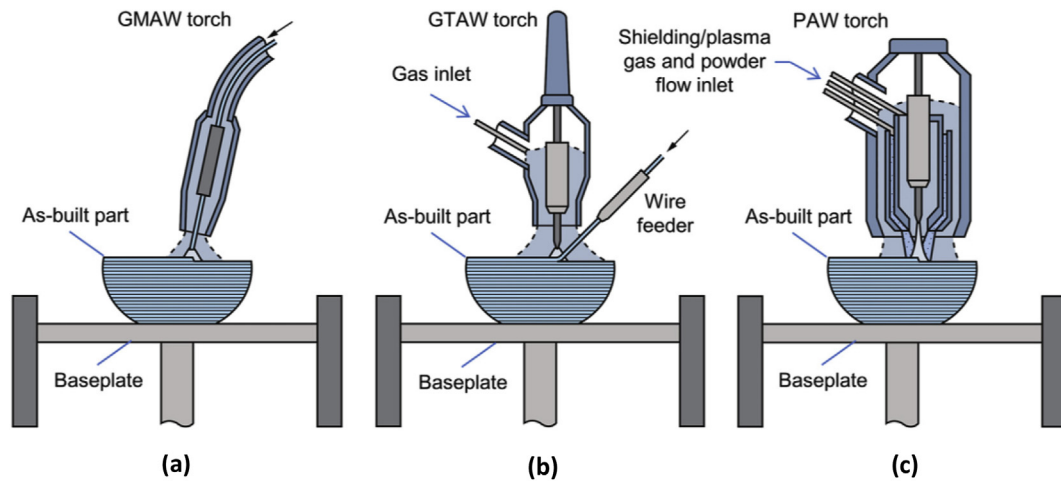


Fig. 5. 2D schematic of (a) GMAW, (b) GTAW, and (c) PAW processes [38].

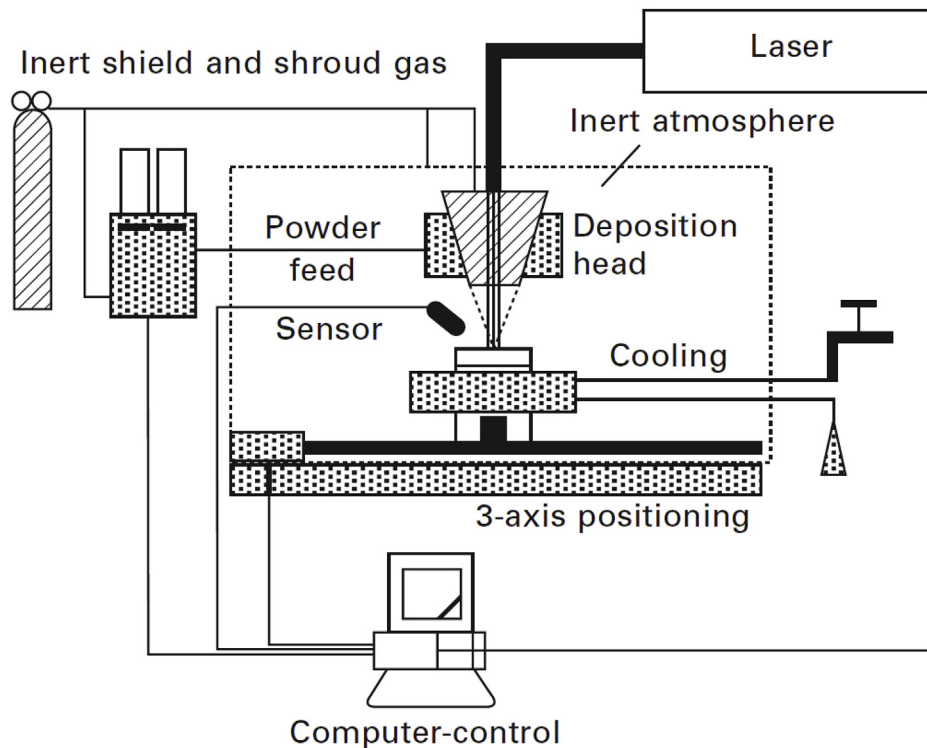


Fig. 6. 2D schematic of LDMD process [42].

product's quality. In this process, the same or different compositions can be used for the build material and substrate. First, a small molten powder is absorbed by focusing laser into the substrate in an enclosing chamber. The powder is fed into the pool by an inert gas stream simultaneously. Then, the laser starts to melt the deposited powder and build the part layer by layer. The molten powder is cooled down and solidified step by step. The process is repeated until the product is finished. The nozzle is a vital component in LDMD due to its impacts on surface roughness and hardness. Hence, the design of the extruder is important to achieve high-quality products. The nozzles in LDMD consist of a central passage with gas flow, an outlet for powder delivery, and another optional outlet with the gas flow to direct the powder flow to the system [41]. A turbomolecular pump with a gas pressure of 10^{-3} Pa in the chamber is used to vacuum the air for a better printing process. Also, a soft agglomerate breakaway powder is used to cover the final printed sample, and blasting is used to

avoid any contamination after removing the sample from the chamber. The capabilities of DED processes are discussed to find out the process characteristics based on requirements. Controlling unparalleled microstructure, solidification rate, material composition, and vital parameters helps manufacturers to have more freedom in producing metal components. Besides, repairing with high quality, printing dense thin layers, producing in situ composite metals, and making complex medical implants are alternative advantages of the DED process.

3. Research works on DED processes

In this section, a brief description is outlined to understand the capabilities of each DED process. Process parameters and microstructure of each process are discussed to find out the gaps in DED processes. In spite of the wide range of capabilities of DED, a limited range of metal alloys can be used

in this process. DED is capable to print functionally graded materials (FGM). It is a combination of materials in different mass fractions with various material properties. For example, Schneider-Maunoury et al. [43] printed Ti6Al4V–molybdenum alloys from 0 to 100 wt.%. Good adhesion between each layer and substrate was achieved and uniformity in powder mixture was observed as well. Subsequently, by increasing the molybdenum content, the size distribution of equiaxed grains decreased while microhardness increased with the value of 450 HV with 75 wt.%. Costa et al. [44] proposed a thermo-kinetic model with transformation kinetics and quantitative property–structure relationships in Abaqus® to study substrate size and idle time effects on microstructure and hardness of AISI 420 steel in layer powder deposition (LPD). Fresh martensite and austenite were observed for the hard upper section while the lower section accommodated tempered martensite. The amount of tempered martensite was reduced because of heat accumulation during printing.

Powder pre-processing treatments, feed rate, feeding powder into the extruder, and transferring powder between molten pool and nozzle

should be considered before the printing process in LDMD [45]. Saboori et al. [46] found that a constant laser power and an increase in powder feeding rate led to better surface quality and mechanical properties, while choosing a proper distance between nozzle and substrate was also important in material deposition. Delivering powder is dependent on mass flow rate based on acoustic emission and spectrum signals inspection. Wilson et al. [47] repaired and remanufactured turbine blades with 0.03 mm accuracy. Results indicated 45% carbon footprint enhancement and 36% energy saving by repairing 10% volume of the whole part. Various studies have been conducted to improve the surface quality and mechanical properties of 3D printed products in DED processes. Boisse-lier et al. [48] found that the flowability and laser power affected stainless steel AISI316 powder morphology. Also, they showed how defects such as porosity were generated due to the non-optimized process parameters. Shim et al. [49] evaluated the layer and slicing thickness by using the feedback control method in printing metal alloys. Powder feed rate had a direct effect on deposited height, but inhomogeneity of

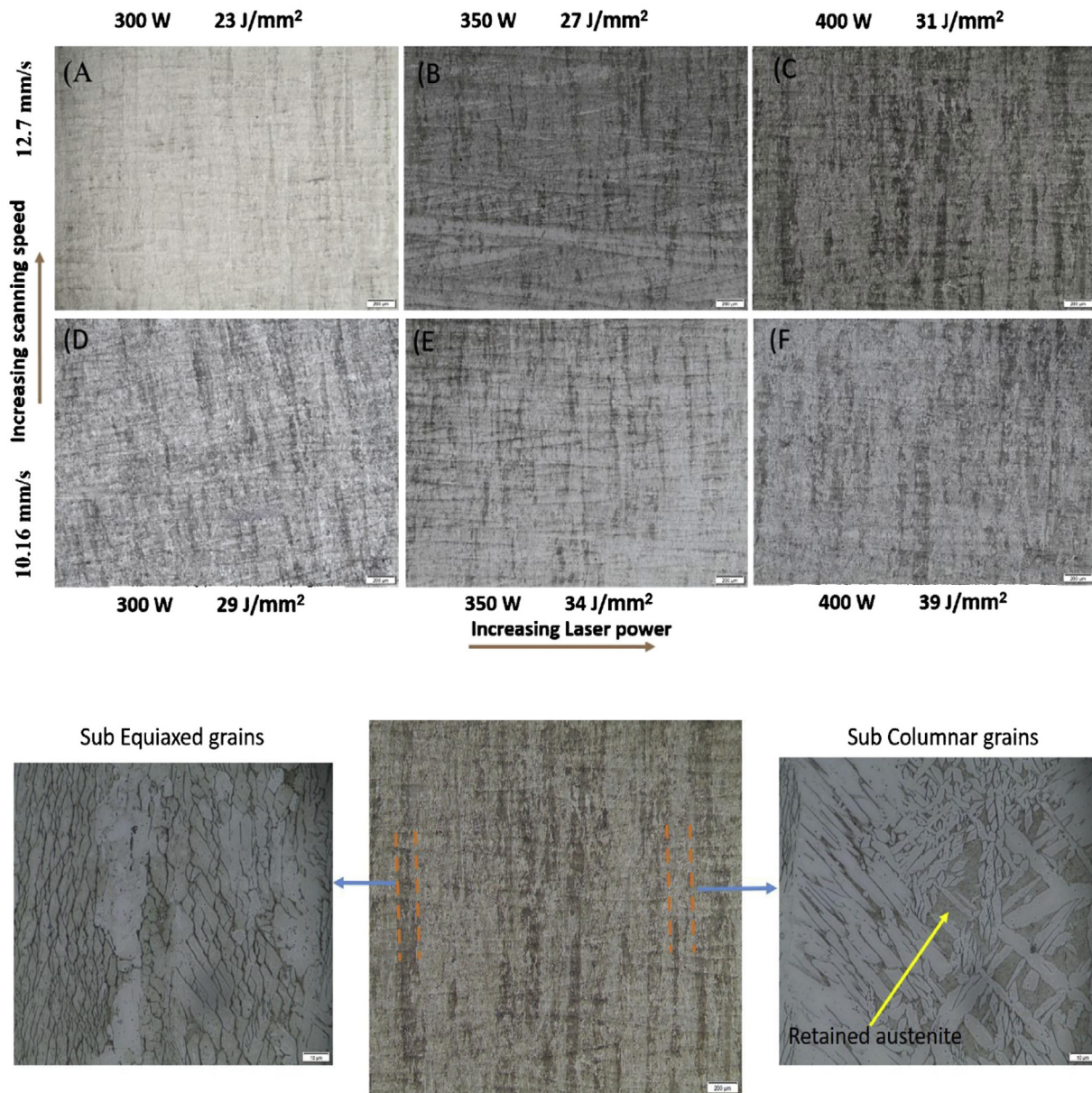


Fig. 7. Microstructure of 17-4 PH samples with different parameters [51].

micro-hardness was observed due to the deposition time. Meanwhile, the best dimensional accuracy and uniform texture were achieved with a stable melting zone in X direction.

Besides, Rombouts et al. [50] investigated the effects of loading orientation and build geometry for Inconel 625 in two different directions, namely, horizontal orientation and vertical orientation. Results showed that the produced Inconel 625 in casting and annealing process had higher elongation but lower tensile strength at a low cooling rate compared to both directions in laser metal deposition (LMD) due to the good heat conduction away from the interaction zone. Also, the low cooling rate and heat accumulation affected the strength of standing orientation because of the higher carbide content. Mathoho et al. [51] studied 17-4 PH stainless steel powder characteristics in the DED process. Various parameters were investigated to find out their effects on porosity, microstructural evolution, microhardness, and corrosion behavior. Each sample showed specific features because of different process parameters. 10.16 mm/s scanning speed and 300 W laser power resulted in 99.9% density and had positive effects on corrosion resistance. As shown in Fig. 7, both martensite and retained austenite were visible. However, the niobium precipitates did not dissolve entirely in homogenizing process at 1100 °C in this research.

Fusion and material binding are different in metal printing, so texture and properties are affected by parameters and their characteristics. The surface is not oxidized so high-purity builds can be achieved in LDMD. Also, this technique has higher deposition rates than others in conductive materials due to the system characteristics. On the other hand, low cooling rate due to the sensitivity of residual magnetic fields, and deflection of the negatively charged laser because of heat transfer by convection, are the weaknesses of this process. Another advantage of DED process is to print multi-material simultaneously. Carroll et al. [52] fabricated and evaluated elemental composition, microstructure, phase composition, and mechanical properties of SS304L stainless steel and

Inconel 625 (see Fig. 8). The samples were printed successfully, but cracks were found in a region composed of 79 wt.% SS304L and 21 wt.% Inconel 625. Ribeiro et al. [53] used a five-axis laser-based DED with a 0.8 mm laser spot to investigate linear, zigzag, chessboard, and contour deposition paths and beads stepover for 316L stainless steel and FGM. Higher values of flatness (4803 μm) and 75 μm SR were obtained at 0.55 mm chessboard stepover while the lowest SR with the value of 37 μm was achieved at 0.44 mm beads stepover and contour path.

Furthermore, Wolff et al. [54] examined the effects of X-ray diffraction, porosity, and fractography of Ti-6Al-4V with different build orientations and laser power on tensile behavior and product strength. The mentioned factors showed that the printed samples in Y direction with 800 W laser power had higher strength and lower porosity compared to the other build directions. In another study, Kakinuma et al. [55] analyzed two types of Inconel 625 powder and found cracks and voids with 2000 W and 1280 W laser power, respectively. Kim et al. [56] realized that 400 W laser power caused crack due to the poor binding in stainless-steel 316L. Increasing scanning speed and power level led to poor fusion for Ti-6Al-4V as well [57]. Also, in this work, 10 mm/s scanning speed and low mass flow rate of powder (10 g/min) could maximize micro-hardness, friction, and modulus in 316L materials.

Moreover, previous research works showed how developments and optimization in WAAM can lead to uniform microstructure in metal products [37]. Usually, GTAW and tungsten inert gas (TIG) welding are used to repair metal components such as dies and cores. Liu et al. [30] achieved uniform welding when the focus point was inside the part. Results indicated that hot wire had a little impact on residual stress when the voltage of hot wire was less than 5 V. Näsström et al. [58] found that lower heat output led to cavities due to the accumulations of unmelted wire. On the other hand, too much heat output caused rougher surfaces, fluctuations, and wider welds. Thus, it is vital to assign optimal conditions to achieve better surface quality and mechanical properties. In another work, Karadeniz et al. [59] found that the penetration was increased by 0.02–0.12 mm for 22–26 V arc voltage in GMAW. Meanwhile, increasing welding speed had a direct effect on penetration and the value of 60 cm/min speed resulted in 0.08 mm penetration. Shi et al. [60] combined SLM and WAAM to examine Ti-6Al-4V interface bonding between each printed layer and bonding in horizontal and vertical orientations with the substrate. Yield strength, ultimate tensile strength (UTS), and elongation of SLM, WAAM, and SLM-WAAM were analyzed accordingly. WAAM specimens showed lower strength compared to SLM and SLM-WAAM. Also, vertical SLM-WAAM parts were stronger compared to horizontal SLM-WAAM with 890 MPa yield strength, 905 MPa UTS, and 10.2% elongation for vertical parts. This is a very interesting finding which is contrary to the vertical SLM parts being weaker than horizontal SLM parts. Syed et al. [61] combined wire and coaxial powder feeding in LDMD to increase the efficiency and quality of printed products. The results indicated that the porosity decreased by 20% compared to the powder method which led to better mechanical properties.

A defect in jointed-arm robotized DED systems is a collision between the head and the build-up part. To overcome this issue part segmentation into sub-parts and joining the elements has been useful solutions. Akbari et al. [62] worked on joining stainless steel (316LSi) with robotized laser/wire directed energy deposition (RLWDED) followed by an autogenous fiber laser welding. As shown in Fig. 9, a six-axis KUKA robot was used. The range of 18–35 μm porosity was found in the welding zone because of the lack of fusion in the specific zone. However, cracks and inclusions were not found in this zone. In brief, the welding quality was good and no negative effects on tensile strength were found. Moreover, Zhang et al. [63] developed a novel ASHM technique by integrating a jointed-arm robotic system of cold metal transfer (CMT)/WAAM and milling, as shown in Fig. 10. A range of 0.4–1.2 mm milling thickness showed major improvement in SR of the produced products with the percentage of 22.9% and 31.6% compared to the conventional WAAM process. In contrast, by increasing the thickness, the surface texture

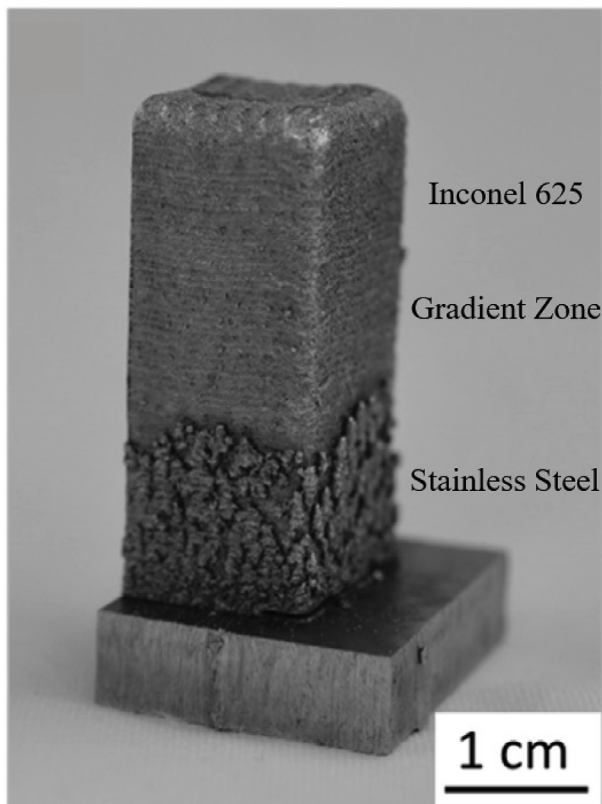


Fig. 8. Photograph of FGM specimen [52].

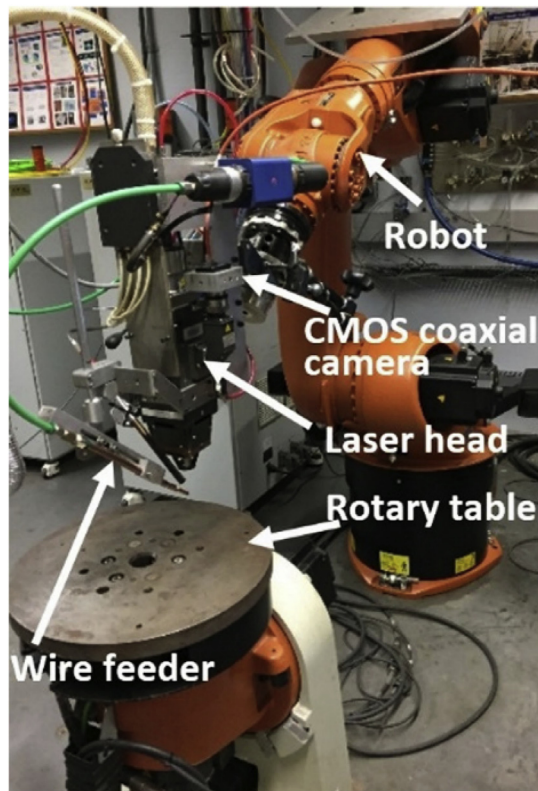


Fig. 9. Components of RLWDED [62].

became poor and rough. In addition, the results illustrated that by changing melt flow, the accuracy improved.

There have been research works on LDMD to find out the effects of process parameters on powder deposition. Piscopo et al. [64] investigated the LDMD parameters of Al2024 aluminum alloy using finite element analysis (FEA) (Abaqus® software) and experimental procedure. They developed a numerical model with an 8% error to predict the deposited material. Also, the results showed that specific energy and laser power had a great effect on melt pool and printing time. Choron et al. [65] examined the printing of Ti-48Al-2Cr-2Nb intermetallic alloy, which has high cracking susceptibility and low thermal shock resistance, by analyzing different cooling conditions and heating treatments. Cracks were found in beads due to the fast cooling after material deposition. This subsequent heat treatment eliminated cracks in microstructure and resulted in a fine and isotropic condition. Gharbi et al. [66] examined the effects of direct metal deposition (DMD) parameters on SR and dimensional accuracy in printed Ti-6Al-4V parts. Waviness and surface roughness were decreased by increasing laser power and laser speed. Agglomerations were caused due to the non-melted particles in the wall

surface. Pant et al. [67] found that 300 W laser power, 4 mm/s scanning speed, and 120 μm layer thickness resulted in better surface quality in printed layers. Zhu et al. [68] investigated the laser focus effects on surface quality in LDMD. Results showed the final part's quality is better by focusing the laser from top to the bottom in the printing process. Besides, -1 mm and 3 mm powder defocusing distance resulted in lower surface waviness with the value of 0.325 mm and 0.702 mm, respectively. However, the process is capable of printing different parts but limitations such as low quality and strength still exist in this method which can be eliminated with five-axis LDMD [69].

Moradi et al. [25] indicated that a 2.5 mm/s scanning speed, 28.52 g/min material flow, and unidirectional scanning pattern led to a smoother surface in 3D printing of Inconel 718 alloy. Ahsan et al. [70] introduced a numerical method with experimental validation for local temperature history, track profile geometry, and grain size. The developed model showed a good agreement in a comparison with the experimental model. As an example, they found that prior- β columnar grain size increased to 500 μm when laser power increased to 1200 W. Wen et al. [71] developed a numerical model by solving the coupled momentum transfer equations to predict and analyze the flow rate and laser interaction. This model was successful in terms of powder deposition, laser intensity, and deposition zone. Laser intensity and its position with the power of 300 W and 0.75 mm beam radius are shown in Fig. 11. In another work conducted by Moradi et al. [72], the width, height, and average grain size increased by increasing laser power while the stability became lower. They found that the quality of deposited metal is affected by changing the focal plane position. However, these factors are important to increase the quality and properties of printed products; higher surface quality cannot be achieved without post-processing techniques.

4. Limitations in DED processes

This section covers the issues and defects that may happen in DED processes. DED processes are capable of building a wide range of products. Different advantages can be achieved due to the process's characteristics. Despite the features that were discussed in the DED section, limitations and defects exist in this technology, as shown in Fig. 12. Material fusion or sintering in DED takes advantage of a focused energy source that is the laser to melt materials in an inert atmosphere. The process is started by pre-heating the build plate or the entire system. Hot isostatic pressing (HIP) is recommended due to the high residual stress in this process. On the other hand, the energy is applied to the narrow region to melt the material and substrate simultaneously. For example, large anisotropy in mechanical properties is another issue that can be analyzed. Grain morphology, crystallographic texture, lack-of-fusion defects, phase transformation, heterogeneous recrystallization are the main factors that affect anisotropy in DED process [73]. Grain elongation in build orientation is high in DED products when their structure is roughly uniform. Stiffness, strength, and ductility under tensile strength are decreased when anisotropy in grain structure corresponds to the poor

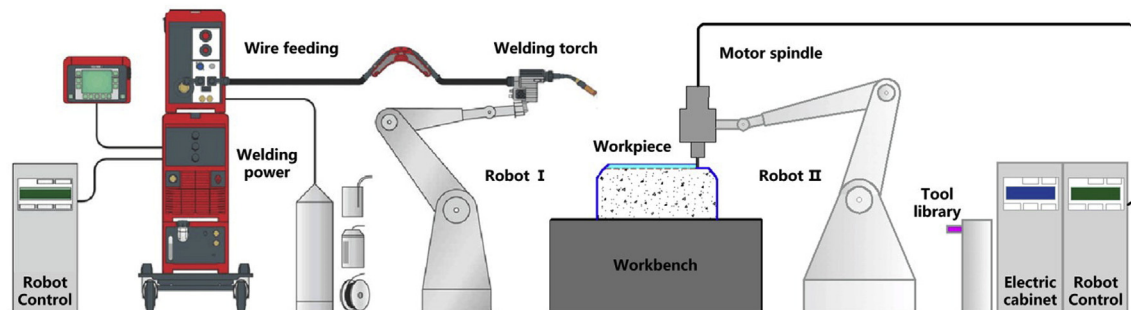


Fig. 10. Schematic of CMT/WAAM and milling [63].

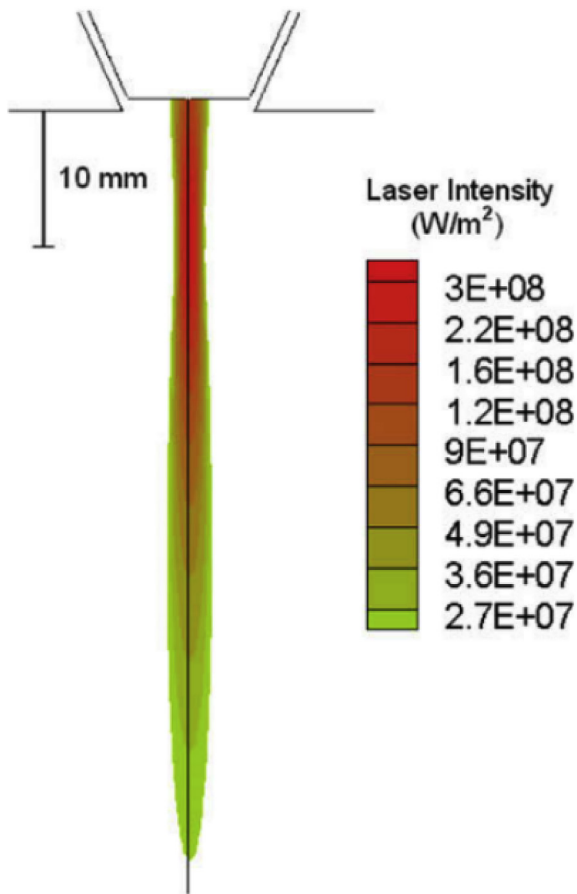


Fig. 11. Numerical model of laser intensity profile [71].

particle distribution. However, post-processing techniques such as machining and HIP can be used to reduce anisotropy.

To achieve the final product's dimension in DED, the process must be repeated layer by layer and this may cause inaccurate deposition or insufficient deposition of material in each layer. Also, due to the layer-by-layer binding nature, the final surface quality is poor or partial bonding may happen [16]. Irregularly broken, elliptic cross-section and non-uniform structure in laser printing might occur due to the instability in or non-optimal melting temperature. Besides, controlling the dimensional accuracy and therefore achieving constant layer growth in DED is difficult. On the other hand, in some cases, post-processing techniques cannot be used due to unavailability and time limitation.

Moreover, distortions, residual stresses, fractures, and rugosity are common defects in metal 3D printing. Sometimes, part distortion and residual stresses are the results of phase transformations and localized heating during the process due to poor flowability. These issues happen in DED due to different heating and cooling zones during the printing and lack of fusion in the microstructure. Porosity is a common drawback in various metals due to the over sintering or non-optimal parameters [74]. Inhomogeneities in printed products also cause porosity in microstructure. Thus, this issue can impact mechanical properties by absorbing water or moisture [75]. Temperature changes, gravity, and capillary forces lead to porosity and warping [76].

Furthermore, shrinkage, lack of fusion, and non-optimal material flow rate cause irregular pores which can be detected in the scanning electron microscope (SEM) analysis [77,78]. High distortion and residual stress can be affected by the complexity of the sample. These issues affect mechanical properties and material fusion during the printing process. As an example, for aluminum alloy 6061, 700 °C preheating can reduce residual stress and final distortion up to 80.2% and 90.1%, respectively. In the DED process, melt pool geometry controls the resolution which is affected by parameters while in wire-based DED process resolution is determined by feedstock delivery. Errors may occur by assigning non-optimized changes in stand-off distance between substrate and feedstock outlet. Thus, melt-pool geometry is changed and this leads to

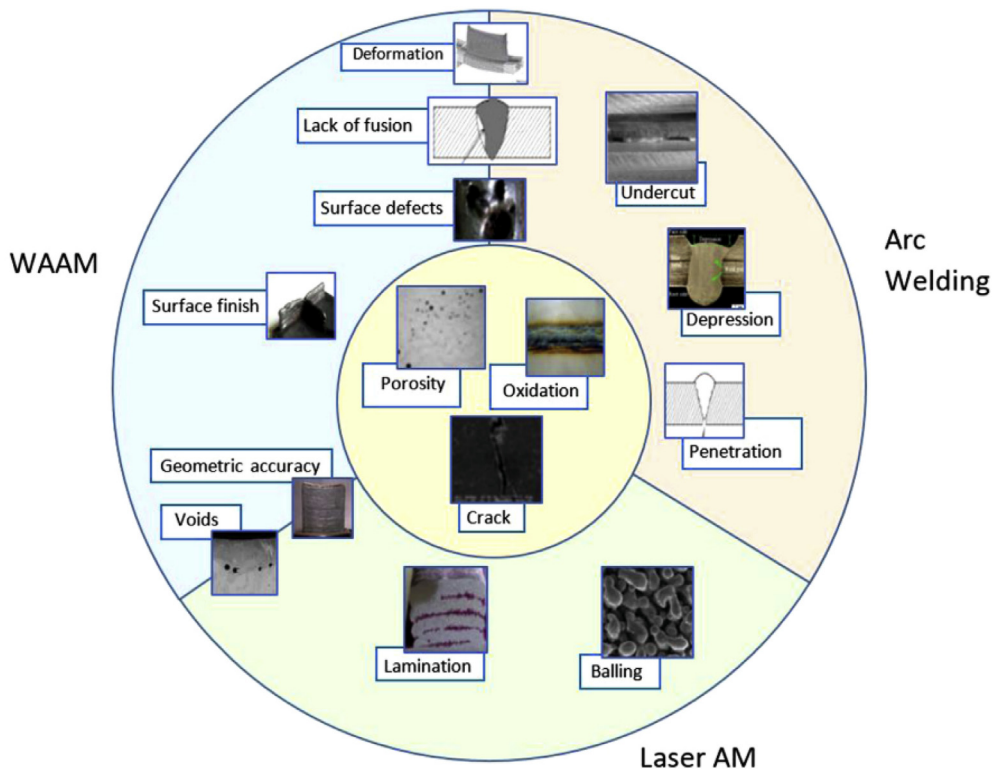


Fig. 12. Defects in DED processes [80].

discussed defects and issues such as delamination [79]. As an example, the defects of DED process after printing of 316L materials with different scanning speeds can be seen in Fig. 13.

Furthermore, dishing, humping, and balling of the solidified area occur by surface tensions and temperature gradients during printing. Moreover, long printing processes, errors in post-processing technologies, low process accuracy after printing, and material waste are the main problems in using secondary processes. Thus, the final cost would be high and the industries are not able to reduce cost, scrap, and processing time. In addition, using support structure in metal 3D printing is costly and increases the printing time. In addition, by removing supports, the surface texture is affected and support separation may damage the surface or collapse the product. Therefore, it is suggested to assign proper parameters to minimize the use of supports. Staircase defect is another defect due to the layer-by-layer printing in AM which leads to poor surface quality. Thus, post-processing or HM is a potential way to eliminate poor surface finish, long cycle time, and poor adhesion.

5. Subtractive hybrid manufacturing

5.1. Hybrid subtractive manufacturing

Over the past few years, the DED process combined with subtractive manufacturing (SM) or computer numerical control (CNC) has been used to achieve high quality and accuracy in metal products [82,83]. The secondary processes can be classified into subtractive, rolling, peening, and burnishing. Each secondary process can minimize the limitations of the other one and add advantages to the AM system [84]. These technologies can be used to build products from micro to large-scale made of metals, plastics, or hydrogels [85–87]. One of the efficient and flexible strategies to increase productivity and quality, reduce leading time, and meet the demand of customization is hybridization [88,89]. Increasing build rates, build volumes, and reducing the machine changes are the positive aspects of ASHM over AM [90]. Liu et al. [91] and Mognol et al. [92] made a comparison to investigate the differences between AM and subtractive technologies. Combining AM and SM to produce metallic components is trending these days. Machining and metal deposition are common processes in HM but few types of research were examined in a combination of FDM and machining process [93].

ASHM is useful to reduce additional movements by retaining the part clamping position during the process [94]. This means the time to

produce products and material waste decrease as well [95]. As an example, mold components such as core and cavity can be built by the HM process. In addition, another advantage that is highly effective in product development is that unreachable areas in traditional post-processing techniques can be machined by using this technology. Meanwhile, eliminating support structures can be done by developing a multi-axis system or jointed-arm robots without any secondary process [96].

High precise surface texture and manipulation of the materials' microstructure can be achieved by rolling, machining, and ultrasonic. As an example, Hodonou et al. [97] developed a systematic methodology by using fuzzy logic to find out the differences between AM and SM processes and cost and environmental effects to select appropriate additive or SM processes. Results indicated that economists prefer machining while neutrals and environmentalists select AM as a capable process to manufacture products [98]. In fact, by combining these technologies, it would be possible to repair metal components with less cost in HM [99].

Process parameters, technology integration, solid production, and series production are the four phases of HM. After achieving these phases, programming, main process, and part separation are the sections of HM that need to be identified [100]. CAD models converted to the G-codes and tool paths are generated based on requirements in subtractive and additive processes. After that, the operations are conducted automatically between these two processes. Therefore, the product is built by adding material and milling process [101]. Free conversion between five-axis milling and laser printing is a common way to be used in ASHM. To achieve high-quality hybrid machining, the printing process in the initial step should deposit excessive material to have more freedom in the machining process. This can be done by generating a larger offset on the whole sample by the controller. It should be noted that this overbuilding and offset should be minimized, otherwise the process's cost would increase due to the high cost of feedstock.

Additionally, over the regions that need high accuracy, machining such as milling can be done simultaneously or after the printing process. Planning operations in ASHM are reduced while more machine tools are needed to have a stable hybrid process. Clamping to keep the sample in place and increase the accuracy with high repeatability is also important in ASHM [102]. Finally, the product is ready as an end-user or prototype part. Similar to the AM, build orientation is also effective on a surface texture in ASHM. Higher freedom in tool motion and material deposition to decrease collision and defects are highly important for better accessibility and part decomposition

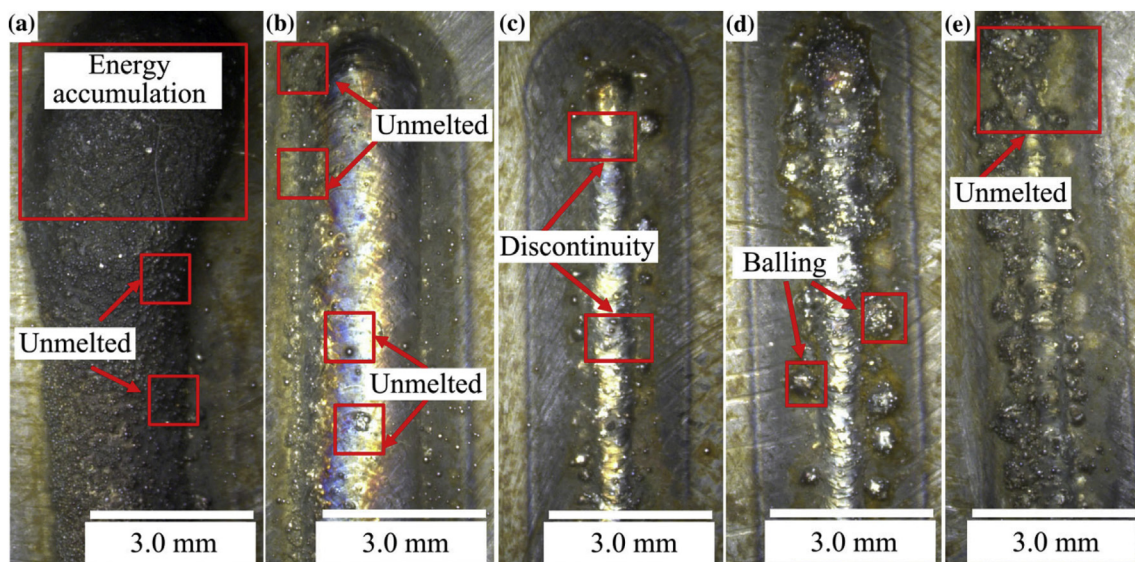


Fig. 13. Defects of printed 316L with scanning speed of (a) 280 mm/min, (b) 360 mm/min, (c) 440 mm/min, (d) 520 mm/min, and (e) 600 mm/min, and constant $P = 1000$ W [81].

in HM. A novel job routings algorithm was created by Strong et al. [103] to optimize the process planning of HM. Performance improvement was conducted by this algorithm as a process plan. Nassehi et al. [104] developed a model for constructing highly complex products with HM and showed its capability in increasing productivity. Soshi et al. [105] used DED and subtractive machining to produce a mold by using a framed grid. The results indicated a short cycle time in produced mold and 45% cooling efficiency.

Benoist et al. [106] developed an algorithm associated with Inspire® and Abaqus® for topology optimization of hydraulic block in hybrid additive/subtractive process. Results showed that the algorithm was highly effective to reduce cutting forces in machining and optimize process parameters of the DED process to achieve cheaper final parts, lower material consumption, and lighter hydraulic block by optimizing constraint, machining, thermal features, and assembly. Kerbrat et al. [107] used the design for manufacturing (DFM) method for powder-based technologies and SM. Obstacles in manufacturing due to the expensive materials, complex features, and poor quality were eliminated significantly. Patterson et al. [108] proposed a new perspective in design and topology optimization (TO) for hybrid additive manufacturing (HAM) to integrate the design phase and manufacturing procedure. TO is a powerful method to decrease scrap and material waste and achieve the optimum design. Expensive materials, system issues, poor accuracy, and non-satisfactory design are the main aims that encourage engineers to implement TO as pre-processing technique to increase strength and stiffness without sacrificing product [109]. TO is also effective to reduce trial and error in design and manufacturing procedures. This method can be widely used for different applications such as casting and molding and is dependent on layers and feature fitting [110]. Path planning and a combination of patterns and contour offset are important elements in TO [111]. In this review, details are presented to identify the gaps and features of these processes in ASHM of DED processes. In the following sections, overviews on HM of DED processes are presented.

5.2. Hybridization of DED with a subtractive process

DED hybridization process consists of DED and mechanical machining processes. The laser beam focuses on metal powder to sinter them layer by layer. Subsequently, the process is repeated several times until the end. Meanwhile, subtractive technologies such as CNC machining can be assigned to the machine to remove or modify the product during 3D printing procedure. The machine follows generated G-code which is developed by exclusive software. Material is deposited from the bottom to the top. After depositing the first few layers, the hybrid system enables the subtractive process to machine sample where the DED process is not able to deposit material. Both 3D printing and machining can work simultaneously in this system to achieve the highest quality of metallic products. For example, the system is able to machine the rough surfaces after the layers are deposited to have a uniform texture. However, the joint system can work separately. As an example, after finishing the printing procedure, the machining section starts to remove excessive material from printed product to make the surface smooth and eliminate errors. Workstations are available and evolved based on machining in three axes or more based on needs. Poor accuracy and bonding, deformation, and limited material feedstock in wire-based DED make the laser-based process on-demand [112]. Research works have been done on this technology; for example, a comprehensive review was conducted on the DED process and SM by Dávila et al. [113]. Kerschbaumer et al. [114] produced samples by using a five-axis machine with high strength and good quality without post-processing technique and heat treatment. Liou et al. [115] worked on the hybrid deposition-machining process with a quantitative understanding of dependant and independent parameters.

Laser beam diameter and laser power were the most important elements. Results showed that by increasing scanning speed, layer thickness increased while layer thickness is related to power density and powder feed rate as well. Layer thickness, surface roughness, and processing time

were considered as main dependent parameters. Controlling and optimizing these factors (e.g., laser power, cutting speed, layer thickness, spindle speed, and temperature) are vital in enhancing printed parts. Also, controlling residual stresses can be done by milling parameters in HM that lead to greater compressive strength and better surface quality. In contrast, this issue can be minimized in DED due to the capability of controlling powder feed rate.

Specific computer-aided manufacturing software applications such as Siemens NX, MasterCAM, and PowerMill are used to generate a path for milling cutters. The machines have vertical three axes or five axes to remove material while the DED process deposits material on the substrate. As shown in Fig. 14(a)–(d), different combinations of DED and conventional machining depict how these processes work to finish a product. The laser scanning system must be optimized to avoid structural collision with the CNC milling spindle. Defects appear due to the poor layer binding and voids between layers. Hence, better properties and quality can be achieved by assigning proper parameters. For example, Yamazaki [116] investigated the tensile strength of Inconel 718 material and the 316S31 substrate in a five-axis INTEGREX i-400 HM machine. Results illustrated that joint strength was higher compared to 316S31 material. Fig. 14(e) and (f) shows a production chain of ASHM of DED process for metallic components with a few examples.

Moreover, material deposition can be modified to achieve the highest accuracy in ASHM process. For example, Zhang et al. [120] proposed a novel strategy to deposit the optimal amount of stainless steel 316L material by using simulation and experimental procedure to improve the capability of the hybrid manufacturing process and dimensional accuracy. MATLAB simulation was used to predict the planer's height and stepover. This technique was useful for different material depositions and showed that the deposition time decreased by increasing feed rate, laser power, and powder flow rate in the DED process. Xie et al. [121] worked on a combination of DED and machining processes to analyze parameters and examined their effects on hardened stainless steel to produce complex aviation bearing brackets. Simulation in Abaqus® was applied to examining the optimum range of processes' parameters. The range of 100–150 m/min milling speed, 0.01–0.02 mm/z feed per tooth, and 0.1–0.15 mm cutting depth were the optimal conditions. In the DED process, 1000–1200 W, 0.01–0.02 m/s, and 2–3 mm were proper ranges for laser power, scanning speed and spot diameter, respectively.

Chen et al. [122] developed a five-axis milling and DED machine and found that temperature and residual stress influenced the geometry. Heigel et al. [123] studied scan strategy, heat-treatment, and machining strategy in ASHM to understand their effects on distortion. Thermal processing caused stress distribution due to the compression between layers after solidifying. Heat treatment was an effective way to reduce the residual stresses. Phase transformation, which changed stress balance, was a result of machining. Thus, by predicting and analyzing these factors, more accurate and precise parts can be made.

Liou et al. [124] used a five-axis laser deposition system (Rofin-Sinar 025) and a CNC milling machine system (Fadal VMC-3016L) to build complex metal parts. Material flow in DED changed the surface quality and had effects on laser efficiency. Moreover, dividing parts into subparts was a potential way in process planning for part decomposition to remove support structure and overcome collision. Ren et al. [125] studied the capability of five-axis hybrid manufacturing in repairing damages and corroded texture in die. Zigzag toolpath improved surface texture and waviness of damaged area. In contrast, limitations were observed like reloading the sample because damages were not on one side. Another drawback was porosity or bad surface evenness which affected contour offsetting and therefore deposition quality was not perfect.

In other studies [126,127], authors examined different aspects of ASHM by a combination of arc hybrid layer manufacturing (ArchLM) and CNC machining. Based on process planning, HLM was faster in route and cheaper compared to CNC. A better resolution was conducted when the filler wire was thinner. Heat treatment was also crucial to minimizing

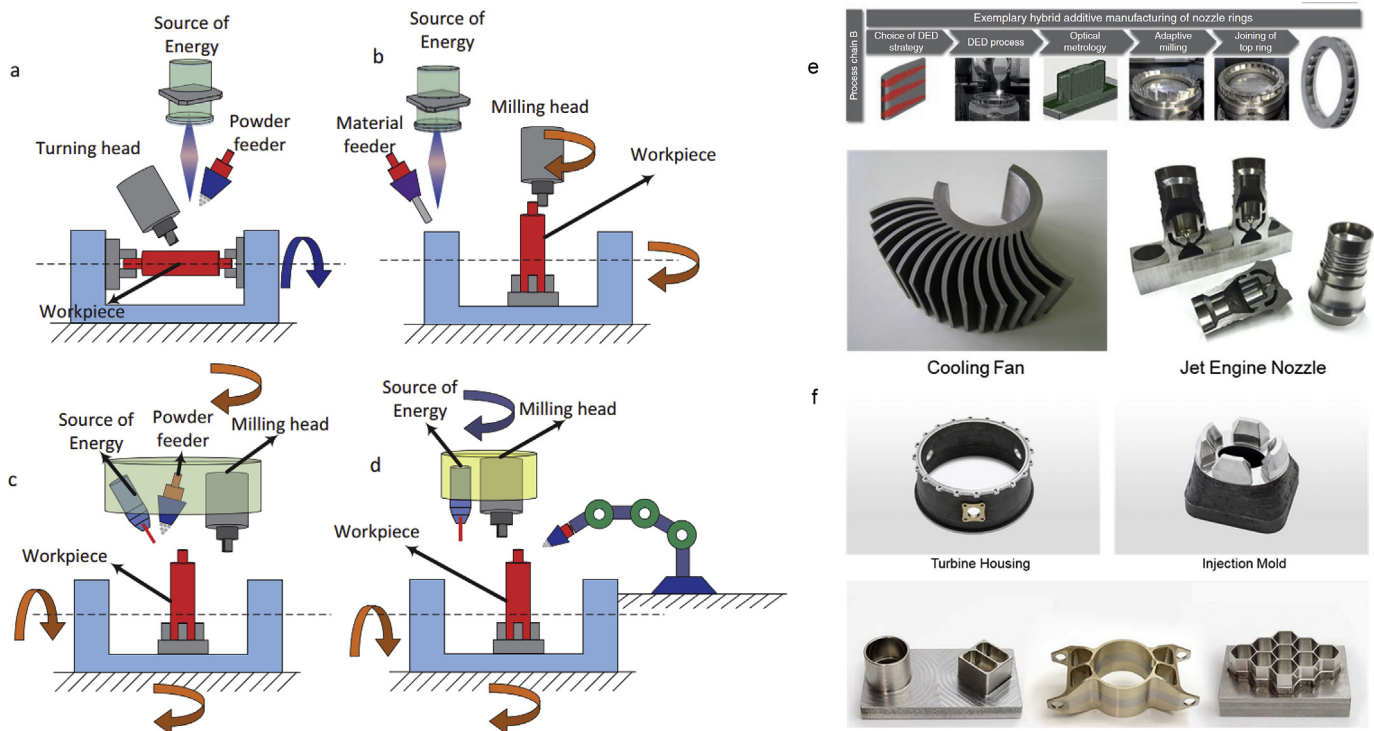


Fig. 14. Hybridization of DED process with (a) turning, (b) multi-axis milling, (c) integrated milling system, and (d) separated multi-axis milling system [117]. (e) The process chain of hybrid DED process for bearing part. Hybrid hexagonal structure product [118]. (f) Example of produced products with hybrid DED system [119].

distortions and residual stresses. Sreenathbabu et al. [128] applied statistical signal-to-noise (S/N) ratio and experimental analysis to determine the optimum parameters of the combined metal active gas (MAG) welding process and CNC machining to improve surface quality and accuracy. Weld voltage led to the higher arc energy and had effects on heat input while weld speed had a small impact on bead width. Yang et al. [129] investigated various aspects of ASHM in producing metal components. They concluded that hardness and residual stress were improved by the rapid cooling process. Results showed that smoother surface texture was achieved compared to the DED process. However, the microstructures of the bottom, middle, and top zones of samples were different (see Fig. 15). This means that the microstructure can be varied which leads to poor properties and quality. Based on provided details, few dendrites can be seen in the bottom zone due to the high cooling and solidification rate at this point. Meanwhile, uniform dendritic grain was found in the middle zone because of lower cooling rate. Also, classical secondary dendrite arms in the top side of machined samples showed more rapid cooling compared to other areas (see Fig. 16).

Oyelola et al. [130] examined the machinability of DED printed Ti-6Al-4V samples to measure the SR and mechanical properties. High machining force was needed for DED parts due to the periodicity and discontinuities in machining while heat treatment reduced cutting forces up to 40% at low cutting speed. They also found that CNC cutting tools affected SR in the DED process. Low values of average SR 0.822 μm and 2.140 μm were obtained for coated and uncoated areas in machining printed parts, respectively [131]. Undoubtedly, SR is affected by a combination of machining tools and printing parameters.

Seidel et al. [132] developed titanium aluminide nozzle for hybrid laser metal deposition and SM. Printing temperature, solidification conditions, and temperature gradient were analyzed to determine the interface crack. They discovered that LMD is a process with a non-homogenous temperature distribution and 600–820 $^{\circ}\text{C}$ brittle-to-ductile transition temperature which led to failure in printing products. Popov et al. [133] investigated the combination of SLM and DED processes with CNC machining. They discovered that the DED

process is more flexible in integration compared to the SLM process in ASHM. Hybridization of SLM is an alternative way to improve surface texture and mechanical properties. However, it is important to define the process planning to eliminate obstacles during the process.

6. Comparison between DED and ASHM processes

6.1. Process parameters and surface quality after machining

There is a relation between surface quality and fatigue in both DED and ASHM processes. Increasing the quality of printed metal parts leads to better mechanical properties. As discussed, the quality of printed products suffers from staircase defects due to the poor binding between each layer. Hence, ASHM can be used as a potential technique to improve surface integrity. The provided details give information that almost all parameters are constant in DED processes while there are some specific features based on process characteristics. Machining or subtractive processes eliminate defects and improve surface quality accordingly. For example, Al-Ahmari et al. [134] machined metal printed products, and the average SR was improved significantly with the value of 0.0085 μm by changing feed rate, spindle speed, and depth of cut.

Chernovol et al. [135] assigned 4.7 m/min wire feed speed, 22 cm/min travel speed, 50 $^{\circ}\text{C}$ interpass temperature, 370 m/min cutting speed, 0.105 mm/tooth feed per tooth, and 1 mm depth of cut to machine ISO 14341-A material in WAAM. The results indicated that the SR improved significantly with the value of 0.395 μm . Also, in another research, the worst SR occurred when the cutting speed was the lowest ($v = 30$ m/min) and feed per tooth was the highest ($fz = 0.0345$ mm/tooth) [136]. Zhang et al. [120] found the optimum DED and milling parameters for 316L material. In hybrid DED, 1800 mm/min feed rate, 24.3 g/min powder flow rate, and 2500 W laser power followed by 12 mm tool diameter, 380 mm/min feed rate, 1600 r/min spindle speed, 60.32 m/min cutting speed, and 1 mm depth of cut achieved the maximum capability of hybrid DED in this study. Zhang et al. [63] achieved major improvements in surface quality by combining WAAM and milling



Fig. 15. Microstructure of ASHM in (a) bottom zone, (b) middle zone, and (c) top zone of the product [129].

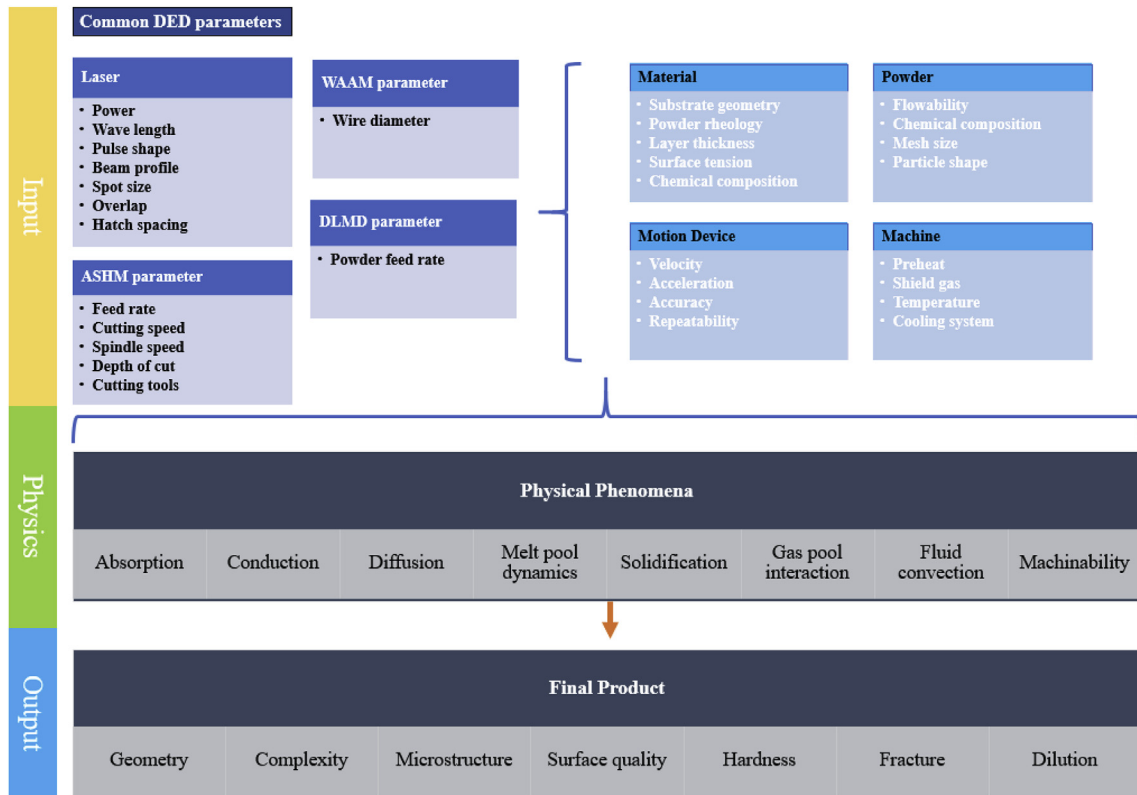


Fig. 16. Input and output parameters of DED and ASHM processes.

process. The assigned parameters (see Table 1) improved SR by 31.6%. As discussed in previous sections, cutting conditions are also important in ASHM based on removing rate. Machining or milling as a secondary process in ASHM leads to better surface integrity without staircase defects compared to the printed products. However, process parameters should be assigned properly to avoid defects such as cracking during machining procedure.

6.2. Mechanical properties and microstructure

In various studies, the mechanical properties of 3D printed metal alloys from titanium to nickel have been investigated to show their characteristics after printing by DED [137,138]. This report focuses on DED processes from WAAM to LDMD as well as ASHM of DED processes. A wide range of materials is available for these technologies while titanium alloys have been analyzed due to their high strength, moderate ductility, good fatigue, and excellent corrosion resistance [139]. Also, this material is one of the most popular ones in DED processes due to the mentioned features [140–142]. This work investigates the condition of the microstructure of printed titanium alloys as well as their properties in DED technologies to find out the capabilities of this process. Data are provided

in form of a table (see Table 2) to analyze and make a comparison between part's properties and DED and ASHM capabilities. In Table 2, UTS, elongation at break, and microstructure conditions of each process are presented to examine the differences. It can be clearly seen that the strength of printed samples is high enough to be used as end-user products. As an example, research works show that the UTS of printed Ti-6Al-4V samples in DED processes is 900–1100 MPa which is close to that of casting and wrought samples.

ASHM affects 3D printed microstructure in terms of hardness and strength. In DED process, the machine uses support structure to build the complex sample. However, due to the attachment of support structure to the main part, deformities and non-uniform surface may occur which affect residual stresses and mechanical properties [113]. ASHM helps to eliminate support structure in complex products. Thus, the texture and microstructure of sample become uniform. During DED process, heating and cooling play an important role in solidification in various zones. Poor adhesion and bonding in small sections and complex features cause residual stress between layers. This issue promotes the formation of cracks and fractures while adaptive controlling of a combination of HM and DED leads to overcoming this issue to avoid poor adhesion between layers by machining the complex zones simultaneously. In addition, thermal discontinuity and

Table 1
Parameters of hybrid WAAM/Milling manufacturing [63].

Parameter	Value
Wire filling speed (m/min)	5.5
Scanning speed (mm/s)	8
Arc current (A)	127
Arc voltage (V)	17.5
Feed rate (mm/s)	25
Spindle speed (r/min)	12000
Milling thickness (mm)	0, 0.4, 0.8, 1.2, 1.6

non-uniformity between layers cause porosity due to the non-optimal binding between layers in DED process. Hence, the standoff distance incrementally is changed layer by layer. ASHM creates a known datum during machining for the following layers. This means that the machining procedure recovers the poor deposit layer simultaneously [143].

Results indicate WAAM and ASHM of DED processes are capable of producing strong materials with high quality. Details show that both DED processes and ASHM are reliable processes to produce metal alloys compared to the cast and wrought processes. The UTS of the produced samples is significantly larger compared to traditional processes. Besides, heat treatment after printing can be an alternative option to increase strength and ductility. The results indicate that by using the ASHM process, the elongation at break improved by 71%, and the porosity reduced by 81%. However, the ASHM improved quality and surface integrity, but its effects on microstructure and strength are not significant based on recorded values for 316L SS material. As shown in Fig. 17, by using kernel average misorientation (KAM), the microstructure of printed and hybrid samples was almost similar [143]. This means that subtractive processes affect surface quality while the effects of machining on microstructure can be neglected.

6.3. Cost and time

ASHM of DED process has many advantages over DED and post-processing techniques in terms of better mechanical properties and surface integrity. However, when it comes to the production line, time and cost are vital factors that enthusiast manufacturers to work with production developments [170]. A generalized statement about the cost of the investigated ASHM demand is extrapolated as a function of the machine tools and material waste. As mentioned in previous sections, using ASHM instead of DED and post-processing techniques aids to decrease the wastage of metal materials up to 97% [122,171]. As an example, the production of metal alloys such as Ti-6Al-4V is expensive in DED process. Also, secondary processes such as machining on printed products lead to more waste that is not reusable after printing. The ASHM process decreases the material waste by eliminating support structure and reducing material deposition in different zones. Wippermann et al. [172] found that using hybrid system in producing products consumes less energy and processing time compared to the conventional systems. Thus, by implementing HM in DED process, the processing time decreases as well due to the less material deposition. In another study, Liu et al. [173] made a comparison between conventional technologies and ASHM. They found that the material waste and time reduced significantly, and energy consumption decreased by 84%.

Manogharan et al. [174] compared the price of AM and ASHM in producing Ti-6Al-4V metallic products. In this case study, they discovered that the price of hybrid system products is not as high as that of post-processing and AM techniques when it comes to higher production volume, while the time to produce products is shorter. A single setup is used for ASHM, which makes the procedure faster compared to the DED process [175]. The usage of material is less because the machine enables the user to produce a product in the same machine. This means that the workload of the equipment for material handling is decreased as well. In addition, since the machine is hybrid, the space due to the less number of machines is less occupied. In brief, ASHM produces product faster with

less energy consumption and the final products is cheaper than AM process [176]. By looking at these advantages, ASHM renders itself a reliable technology to be used in industrial sectors.

7. Summary and challenges in ASHM of DED process

The advantages and disadvantages of AM and HM in producing metal parts are discussed. Although HM brings many advantages regarding product development, limitations still exist in this technology. For instance, cutting fluids in contact with powder materials can be explosive. Moreover, the mixture of these two can be abrasive which would affect the final quality and dimensional accuracy of printed products. Due to the mixture of powder and fluid, particles may act like barrel finishing process. Hence, the mixture abrades the surface of product. In ASHM, the mixture of cutting fluids with powder material leads to changing the cutting conditions due to their effects on heating. This means that fluid makes the heating area cooler and affects machining parameters. In addition, challenges still need to be identified in software and hardware integration such as real-time controlling and cloud manufacturing to gain better and more accurate results. Until now, all experiments have focused on product development and improvements in processes [143,177]. However, limitations still exist in ASHM that need to be eliminated to achieve smooth surface. Besides, cutting tools may crack due to the wrong parameters in the milling process or unwanted defects that happen in the product because of the bad powder feeding rate in laser DED. Mechanical machining also has various factors that should be identified. As an example, choosing a suitable machining tool is vital to reaching high quality after metal deposition. Stainless steel and solid carbide cutting tools are highly effective in machining metal alloys [178].

Controlling the residual stress should be investigated as well to achieve high integrity in microstructural features. Furthermore, the machining process has defects such as balancing the tool holder, excessive tool wear, and scratch on surface quality. Mentioned research works showed that better strength and stiffness are possible when small particle distribution is uniform in DED process. Process parameters in AM were investigated and laser power was the most important factor in fusing powder or wire materials [179]. Build inclination affected surface quality and parts' strength. Perpendicular parts (e.g., printed samples in 30°, 60°, and 75° build angle) had lower strength compared to horizontal and vertical directions (90° build angle) [180]. Part density was affected by powder feed rate and melt pool shape [181]. Higher density leads to better stiffness and lower porosity in final products. In contrast, agglomeration may happen due to the excess of metal particles in specific areas [182,183]. Besides, metal printing limitations such as porosity, delamination, internal fatigues (e.g., crack initiation and crack growth), and staircase are crucial in decreasing mechanical properties. Partial melting is also effective to determine the characteristic of melted material. Poor binding occurs due to the unfused layers and partial melting. Hence, the stiffness and strength of the printed parts become lower. Nevertheless, these works have shown that DED is capable of printing a range of metal alloys for different applications.

Future works can focus on improving mechanical properties through optimization of volume fraction and particle size. Besides, the mechanism of HM in producing hybrid composites in terms of thermal conductivity and dimensional stability should be investigated accordingly. ASHM has shown how this technology is capable of eliminating DED limitations such as balling and accumulation. Table 3 shows differences between AM and ASHM regarding strengths and weaknesses. Developments in a machine into five-axis or jointed arm robots were discussed. Studies indicated that major improvements were achieved by using the ASHM machine. The better surface texture leads to a uniform structure. Uniformity can make the part stronger such that cracks and failures are eliminated. The capabilities of HM of DED process have been discussed, and researchers have shown the reliability and profitability of HM in economic sections to eliminate problems such as expensive materials [136,184].

HM machines are reliable technologies due to their high capability in

Table 2
Microstructure, UTS, and printing condition.

Process	Material	Microstructure	Condition	UTS (MPa)	EL (%)	Ref.	
GTAW	Ti-6Al-4V	Columnar prior β grains + Widmanstätten α/β	AF	929 \pm 41 ^a 965 \pm 39 ^b	9 \pm 1.2 ^a 9 \pm 1 ^b	[144]	
	Inconel 625 Ti-6Al-4V	Coarser Laves particles + Nb precipitates α phase lamella basket weave structures	HT (980 °C) AF	802 ^a 939 \pm 24 ^a 1033 \pm 32 ^b	42 ^a 16 \pm 3 ^a 7.8 \pm 2.3 ^b	[145] [146]	
	Ti-6Al-4V	Lamellar structure	HT (600 °C/4 h/FC)	972 \pm 41 ^a 977 \pm 14 ^b	12.5 \pm 2.5 ^a 6 \pm 3 ^b		
	Ti-6Al-4V	Lamellar structure	HT (834 °C/2 h/FC)	931 \pm 19 ^a 971 \pm 28 ^b	21 \pm 2 ^a 14 \pm 2 ^b		
	Ti-6Al-4V	Widmanstätten α + banded coarsened lamellar α	AF	918 \pm 17 ^a 1033 \pm 19 ^b	14.8 ^a 11.7 ^b	[147]	
	Ti-6Al-4V	/	AF	937 \pm 21 ^a 963 \pm 22 ^b	16.5 \pm 2.7 ^a 7.8 \pm 2 ^b	[148]	
	Al 5083	Columnar grains	AF	296 ^a	17.13 ^a	[149]	
	316L SS	Semicircle morphology + austenite columnar grains	AF	560 \pm 25 ^{a,b}	30 \pm 10 ^{a,b}	[150]	
	GMAW	Inconel 718	Nb precipitates + dendritic structure	AF	828 \pm 8 ^a	28 \pm 2 ^a	[151]
	Al 5083	Columnar grains	AF	269 ^a	10.23 ^a	[149]	
PAW	308L SS	Dendrites of austenite growing vertically + residual ferrite existing	AF	552.95 \pm 4.96 ^{a,b}	54.13 \pm 1.29 ^{a,b}	[152]	
	316L SS	Delta-ferrite (δ) + Vermicular morphology + austenite (γ) matrix	AF	630 ^a	52 \pm 3 ^a	[153]	
PAW	Ti-6Al-4V	Prior columnar β + Martensite α'	AF	988 \pm 19.2 ^b	7 \pm 0.5 ^b	[154]	
	Ti-6Al-4V	Columnar β + martensite α'	AF	968 \pm 12.6 ^b	11.5 \pm 0.5 ^b	[155]	
DLMD	Inconel 625	Laves phase + NbC carbides	IC	771 ^a	50 ^a	[156]	
	Ti-6Al-4V	Columnar grains + martensitic needle structure + a small fraction of β phase	HIP	1025 ^a 1025 ^b	5 ^a 12 ^b	[157]	
	Ti-6Al-4V	Grain structure + Widmanstätten microstructure	HT (970 °C/1 h)	941 ^a 973 ^b	11.6 ^a 10 ^b	[158]	
	Ti-6Al-4V	Columnar β grains + acicular α' martensite	AF	1099 \pm 2 ^a	12.3 ^a	[46]	
	Ti-6Al-4V	Columnar β grains + Widmanstätten (basket weave) platelet α	AF	911 \pm 10 ^a	11.9 ^a	[159]	
	Ti-6Al-4V	epitaxial columnar β cellular+ grains + α' martensitic	AF	902.1	12.5	[160]	
	Ti-6Al-4V	epitaxial columnar β cellular+ grains + α' martensitic	HT (960 °C/2 h)	921.6	16.4	[160]	
	Al 2024	α -Al + CuAl ₂ + Columnar crystals + equiaxed crystals formed	AF	274 \pm 2 ^a 276 \pm 5 ^b	8 \pm 2 ^a 18 \pm 3 ^b	[161]	
	316L SS	Residual δ -ferrite+ austenitic dendrites + columnar grains	AF	624 \pm 10 ^{67°} 649 \pm 2 ^{90°}	17 \pm 3 ^{67°} 23 \pm 3 ^{90°}	[162]	
	316L SS	Micro-cavities + porosities	AF	650 \pm 15 ^a	/	[163]	
	304L SS	/	AF	670 ^a 730 ^b	70 ^a 51 ^b	[164]	
	AISI 316L	Large dendritic grains	AF	770 ^{90°} 900 ^{0°}	4 ^{90°} 6.5 ^{0°}	[165]	
	316 SS	Slender dendrites growing	AF	639 ^b 526 ^a	21 ^b 46 ^a	[166]	
	ASHM	Inconel 625	Small dendrites	Machined/DLMD	751	37	[167]
		316 SS	Slender dendrites growing	Machined/DLMD	587 ^b 689 ^a	59 ^b 29 ^a	[166]
316L SS		Small dendrites	Machined/DLMD	520	27	[167]	
316L SS		Martensite	Machined	600 \pm 10 ^a	40 \pm 10 ^a	[143]	
316L SS		Forming + no changes in microstructure		550 \pm 30 ^b	30 \pm 15 ^b		
316L SS		Increase of primary dendrite and grain size	*159 J/mm ³ 222 J/mm ³ 278 J/mm ³ 370 J/mm ³	562.7 601.6 584.3 570.5	/	[168]	
316L SS		Larger second-phase particles	Machined	429.03 ^a	/	[81]	
Ti-6Al-4V		no difference in grain size	Machined	1163 \pm 35 ^a	/	[169]	
316S31		/	Machined	563	39	[116]	
			WAAM				

AF: as fabricated, HT: heat treated, HIP: hot isostatic pressing, IC: interpass cooling, *: laser energy.

^a In build direction.

^b Orthogonal to build direction.

mass production. Research works on environmental impacts and the use of different coolants have not been investigated yet. Therefore, the effects of the cooling system and environment on mechanical properties in HM should be investigated in the future to fill this gap. Also, it is difficult to build micro features with high accuracy by mechanical machining. Therefore, analysing ASHM products in terms of micro-sized features can be another goal in this topic. Besides, the environmental impacts such as humidity have not been studied on the printed metals. In spite of ASHM capabilities, it is not possible to use a wide range of materials. Hence, working on a combination of metal alloys and composites in ASHM could be done by analysing their characteristics. Also, this work presents the capabilities of ASHM which also can be used for the production of shape

memory alloys with high quality. ASHM improves mechanical and material properties of shape memory alloys by eliminating DED defects. Hence, the actuation of shape memory alloy is enhanced due to the better surface texture and mechanical properties. Besides, future studies could be aligned with industry 4.0 in which intelligent manufacturing is the key in terms of optimization, monitoring, and process planning.

8. Conclusions

The current review extracted the main developments of metal-based materials in DED and HM processes. The advantages and disadvantages of DED and ASHM of DED process were discussed. It was found that

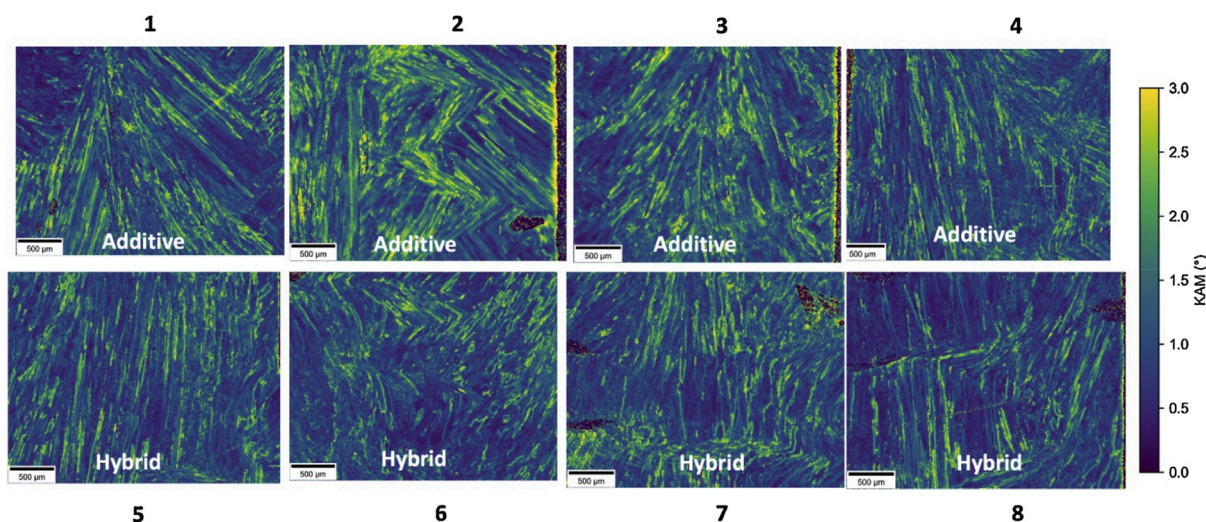


Fig. 17. Kernel Average Misorientation for all printed and machined samples [143].

Table 3

Comparison of DED and ASHM of DED.

Process	DED	ASHM
Principle	A machine that uses a laser to sinter powder or wire to build products layer by layer	A machine that combines DED with other SM processes
Post-processing	Machining, HIP, and EDM are needed to improve surface integrity after 3D printing	No post-processing is needed
Tooling	No tooling during AM process	Tooling is required
Slicing	Uniform slicing	Adaptive slicing
Differences	Geometrical freedom	Customization
	Less accuracy	Geometrical freedom
	Low productivity	High accuracy
	Poor surface quality	High productivity
	High material wastage	Less material wastage
Speed	Low	Faster than AM

ASHM is a potential technique as a substitution for DED because of the combination of two technologies which could remove AM issues. Also, this unique research work showed that DED has different characteristics in printing metal alloys. The novelty of this review work was to show both DED and ASHM of DED simultaneously to elaborate their features and characteristics. From a microscopic view, different microstructures are recorded in DED and ASHM, which leads to different mechanical properties in the final products. Various metal powders were investigated to determine their properties in terms of strength and surface integrity. Delamination, balling effect, poor surface quality, and residual stress are the main issues in both technologies.

Elements like laser power, scan speed, layer thickness, and build inclination were discussed in the metal 3D printing. In both processes, laser power is the energy source that has the greatest effect on material properties. The printed sample has higher strength in vertical and horizontal directions while the lower strength is seen in the perpendicular orientation. Results indicated that the surface texture is improved in the ASHM compared to the AM due to the combination of machining and 3D printing in specific cases. In brief, a combination of AM and subtractive processes paves the path to increase productivity and product development of metal and metal-based composites.

Funding

This research did not receive any specific grant from funding agencies in the public, commercial, or not-for-profit sectors.

Conflict of interest

The authors declare no conflict of interest.

Availability of data and material

The authors confirm that the data supporting this study are available within the article.

Authors' contribution

M. Lalegani Dezaki and M. Bodaghi collected research papers. M. Lalegani Dezaki deduced useful information from these papers under the supervision of A. Serjouei, A. Zolfagharian, M. Fotouhi, M.K.A. Mohd Ariffin, and M. Bodaghi. M. Lalegani Dezaki and M. Bodaghi prepared a draft review paper and A. Serjouei, A. Zolfagharian, M. Fotouhi, M. Moradi and M.K.A. Mohd Ariffin reviewed this paper from the perspectives of correctness, language, and information flow.

Declaration of competing interest

The authors declare that they have no known competing financial interests or personal relationships that could have appeared to influence the work reported in this paper.

References

- [1] Z. Zhu, V.G. Dhokia, A. Nassehi, S.T. Newman, A review of hybrid manufacturing processes – State of the art and future perspectives, *Int. J. Comput. Integr. Manuf.* 26 (2013) 596–615, <https://doi.org/10.1080/0951192X.2012.749530>.
- [2] B. Wang, F. Tao, X. Fang, C. Liu, Y. Liu, T. Freiheit, Smart manufacturing and intelligent manufacturing: A comparative review, *Eng 7* (2021) 738–757, <https://doi.org/10.1016/j.eng.2020.07.017>.
- [3] D.R. Eyers, A.T. Potter, Industrial additive manufacturing: A manufacturing systems perspective, *Comput. Ind.* 92–93 (2017) 208–218, <https://doi.org/10.1016/j.compind.2017.08.002>.

- [4] D. Bourell, J.P. Kruth, M. Leu, G. Levy, D. Rosen, A.M. Beese, A. Clare, Materials for additive manufacturing, *CIRP Ann* 66 (2017) 659–681, <https://doi.org/10.1016/j.cirp.2017.05.009>.
- [5] M. Lalegani Dezaki, M.K.A. Mohd Ariffin, S. Hatami, An overview of fused deposition modelling (FDM): Research, development and process optimisation, *Rapid Prototyp. J.* 27 (2021) 562–582, <https://doi.org/10.1108/RPJ-08-2019-0230>.
- [6] F. Calignano, D. Manfredi, E.P. Ambrosio, S. Biamino, M. Lombardi, E. Atzeni, A. Salmi, P. Minetola, L. Iuliano, P. Fino, Overview on additive manufacturing technologies, *Proc IEEE* 105 (2017) 593–612, <https://doi.org/10.1109/JPROC.2016.2625098>.
- [7] T. Zhang, C.T. Liu, Design of titanium alloys by additive manufacturing: A critical review, *Adv. Powder Mater.* (2021) 100014, <https://doi.org/10.1016/j.apmate.2021.11.001>.
- [8] K.V. Wong, A. Hernandez, A review of additive manufacturing, *ISRN Mech. Eng.* (2012) 208760, <https://doi.org/10.5402/2012/208760>.
- [9] J.S. Cuellar, G. Smit, D. Plettenburg, A. Zadpoor, Additive manufacturing of non-assembly mechanisms, *Addit. Manuf.* 21 (2018) 150–158, <https://doi.org/10.1016/j.addma.2018.02.004>.
- [10] D.S. Thomas, S.W. Gilbert, *Costs and cost effectiveness of additive manufacturing*, Special Publication (NIST SP), National Institute of Standards and Technology, Gaithersburg, MD, Gaithersburg, MD, 2014.
- [11] T.D. Ngo, A. Kashani, G. Imbalzano, K.T.Q. Nguyen, D. Hui, Additive manufacturing (3D printing): A review of materials, methods, applications and challenges, *Compos. B: Eng.* 143 (2018) 172–196, <https://doi.org/10.1016/j.compositesb.2018.02.012>.
- [12] M.M. Dewidar, H.C. Yoon, J.K. Lim, Mechanical properties of metals for biomedical applications using powder metallurgy process: A review, *Met. Mater. Int.* 12 (2006) 193, <https://doi.org/10.1007/BF03027531>.
- [13] S. Sui, Y. Chew, Z. Hao, F. Weng, C. Tan, Z. Du, G. Bi, Effect of cyclic heat treatment on microstructure and mechanical properties of laser aided additive manufacturing Ti–6Al–2Sn–4Zr–2Mo alloy, *Adv. Powder Mater.* (2021) 100002, <https://doi.org/10.1016/j.apmate.2021.09.002>.
- [14] S.H. Ghaffar, J. Corker, M. Fan, Additive manufacturing technology and its implementation in construction as an eco-innovative solution, *Autom. Constr.* 93 (2018) 1–11, <https://doi.org/10.1016/j.autcon.2018.05.005>.
- [15] J. Savolainen, M. Collan, How additive manufacturing technology changes business models? – Review of literature, *Addit. Manuf.* 32 (2020) 101070, <https://doi.org/10.1016/j.addma.2020.101070>.
- [16] A. Suárez, M.J. Tobar, A. Yáñez, I. Pérez, J. Sampedro, V. Amigó, J.J. Candel, Modeling of phase transformations of Ti6Al4V during laser metal deposition, *Phys. Procedia* 12 (2011) 666–673, <https://doi.org/10.1016/j.phpro.2011.03.083>.
- [17] G. Strano, L. Hao, R.M. Everson, K.E. Evans, A new approach to the design and optimisation of support structures in additive manufacturing, *Int. J. Adv. Manuf.* 66 (2013) 1247–1254, <https://doi.org/10.1007/s00170-012-4403-x>.
- [18] N.N. Kumbhar, A. v. Mulay, Post processing methods used to improve surface finish of products which are manufactured by additive manufacturing technologies: A review, *J. Inst. Eng. (India): C* 99 (2018) 481–487, <https://doi.org/10.1007/s40032-016-0340-z>.
- [19] J. Jiang, Y. Ma, Path planning strategies to optimize accuracy, quality, build time and material use in additive manufacturing: A review, *Micromachines (Basel)* 11 (2020), <https://doi.org/10.3390/mi11070633>.
- [20] M. Liu, A. Kumar, S. Bukkapatnam, M. Kuttalamadom, A review of the anomalies in directed energy deposition (DED) processes & potential solutions - Part quality & defects, *Procedia Manuf* 53 (2021) 507–518, <https://doi.org/10.1016/j.promfg.2021.06.093>.
- [21] P. Bajaj, A. Hariharan, A. Kini, P. Kürstner, D. Raabe, E.A. Jäggle, Steels in additive manufacturing: A review of their microstructure and properties, *Mater. Sci. Eng. A* 772 (2020) 138633, <https://doi.org/10.1016/j.msea.2019.138633>.
- [22] A. Jinoop, C. Paul, K. Bindra, Laser-assisted directed energy deposition of nickel super alloys: A review, *Proc. Inst. Mech. Eng. L: J. Mater.: Des. Appl.* 233 (2019) 2376–2400, <https://doi.org/10.1177/1464420719852658>.
- [23] H.J. Yi, J.W. Kim, Y.L. Kim, S. Shin, Effects of cooling rate on the microstructure and tensile properties of wire-arc additive manufactured Ti–6Al–4V alloy, *Met. Mater. Int.* 26 (2020) 1235–1246, <https://doi.org/10.1007/s12540-019-00563-1>.
- [24] A. Saboori, D. Gallo, S. Biamino, P. Fino, M. Lombardi, An overview of additive manufacturing of titanium components by directed energy deposition: microstructure and mechanical properties, *Appl. Sci.* 7 (2017) 883, <https://doi.org/10.3390/app7090883>.
- [25] M. Moradi, A. Hasani, Z. Pourmand, J. Lawrence, Direct laser metal deposition additive manufacturing of Inconel 718 superalloy: Statistical modelling and optimization by design of experiments, *Opt. Laser Technol.* 144 (2021) 107380, <https://doi.org/10.1016/j.optlastec.2021.107380>.
- [26] M. Moradi, A. Hasani, Z. Malekshahi Beiranvand, A. Ashoori, Additive manufacturing of Stellite 6 superalloy by direct laser metal deposition – part 2: Effects of scanning pattern and laser power reduction in different layers, *Opt. Laser Technol.* 131 (2020) 106455, <https://doi.org/10.1016/j.optlastec.2020.106455>.
- [27] T. Makhmutov, N. Razumov, A. Kim, N. Ozerskoy, A. Mazeeva, A. Popovich, Synthesis of CoCrFeNiMnW0.25 high-entropy alloy powders by mechanical alloying and plasma spheroidization processes for additive manufacturing, *Met. Mater. Int.* 27 (2021) 50–54, <https://doi.org/10.1007/s12540-020-00747-0>.
- [28] J. Kranz, D. Herzog, C. Emmelmann, Design guidelines for laser additive manufacturing of lightweight structures in TiAl6V4, *J. Laser Appl.* 27 (2015) S14001, <https://doi.org/10.2351/1.4885235>.
- [29] X. Wang, D. Deng, Y. Hu, F. Ning, H. Wang, W. Cong, H. Zhang, Overhang structure and accuracy in laser engineered net shaping of Fe–Cr steel, *Opt. Laser Technol.* 106 (2018) 357–365, <https://doi.org/10.1016/j.optlastec.2018.04.015>.
- [30] W. Liu, J. Ma, S. Liu, R. Kovacevic, Experimental and numerical investigation of laser hot wire welding, *Int. J. Adv. Manuf.* 78 (2015) 1485–1499, <https://doi.org/10.1007/s00170-014-6756-9>.
- [31] Y. Zhang, D. Yu, J. Zhou, D. Sun, A review of dissimilar welding for titanium alloys with light alloys, *Metall. Res. Technol.* 118 (2021) 213, <https://doi.org/10.1051/metal/2021011>.
- [32] A.R. McAndrew, M. Alvarez Rosales, P.A. Colegrove, J.R. Hönnige, A. Ho, R. Fayolle, K. Eytayo, I. Stan, P. Sukrongpan, A. Crochemore, Z. Pinter, Interpass rolling of Ti–6Al–4V wire + arc additively manufactured features for microstructural refinement, *Addit. Manuf.* 21 (2018) 340–349, <https://doi.org/10.1016/j.addma.2018.03.006>.
- [33] K. Pal, S.K. Pal, Effect of pulse parameters on weld quality in pulsed gas metal arc welding: A review, *J. Mater. Eng. Perform.* 20 (2011) 918–931, <https://doi.org/10.1007/s11665-010-9717-y>.
- [34] A.B. Short, Gas tungsten arc welding of $\alpha + \beta$ titanium alloys: A review, *Mater. Sci. Technol.* 25 (2009) 309–324, <https://doi.org/10.1179/174328408X389463>.
- [35] V.D. Kalyankar, H.V. Naik, Overview of metallurgical studies on weld deposited surface by plasma transferred arc technique, *Mater. Sci. Technol.* 118 (2021) 111, <https://doi.org/10.1051/metal/2020088>.
- [36] J. Zhang, X. Di, C. Li, X. Zhao, L. Ba, X. Jiang, Additive manufacturing of Inconel625-HSLA steel functionally graded material by wire arc additive manufacturing, *Metall. Res. Technol.* 118 (2021) 502, <https://doi.org/10.1051/metal/2021063>.
- [37] B. Wu, Z. Pan, D. Ding, D. Cuiui, H. Li, J. Xu, J. Norrish, A review of the wire arc additive manufacturing of metals: Properties, defects and quality improvement, *J. Manuf. Process.* 35 (2018) 127–139, <https://doi.org/10.1016/j.jmapro.2018.08.001>.
- [38] J.P.M. Pragana, R.F.V. Sampaio, I.M.F. Bragança, C.M.A. Silva, P.A.F. Martins, Hybrid metal additive manufacturing: A state-of-the-art review, *Adv. Ind. Manuf. Eng.* 2 (2021) 100032, <https://doi.org/10.1016/j.aime.2021.100032>.
- [39] P.N. Sibisi, A.P.I. Popoola, N.K.K. Arthur, S.L. Pityana, Review on direct metal laser deposition manufacturing technology for the Ti–6Al–4V alloy, *Int. J. Adv. Manuf.* 107 (2020) 1163–1178, <https://doi.org/10.1007/s00170-019-04851-3>.
- [40] B. Blakey-Milner, P. Gradl, G. Snedden, M. Brooks, J. Pitot, E. Lopez, M. Leary, F. Berto, A. du Plessis, Metal additive manufacturing in aerospace: A review, *Mater. Des.* 209 (2021) 110008, <https://doi.org/10.1016/j.matdes.2021.110008>.
- [41] A.J. Pinkerton, Advances in the modeling of laser direct metal deposition, *J. Laser Appl.* 27 (2015) S15001, <https://doi.org/10.2351/1.4815992>.
- [42] A.J. Pinkerton, Laser direct metal deposition: Theory and applications in manufacturing and maintenance, in: *Lasers Manuf. Mater. Process.*, Elsevier, 2010, pp. 461–491.
- [43] C. Schneider-Maunoury, L. Weiss, P. Acquier, D. Boisselier, P. Laheurte, Functionally graded Ti6Al4V–Mo alloy manufactured with DED-CLAD® process, *Addit. Manuf.* 17 (2017) 55–66, <https://doi.org/10.1016/j.addma.2017.07.008>.
- [44] L. Costa, R. Vilar, T. Reti, A.M. Deus, Rapid tooling by laser powder deposition: process simulation using finite element analysis, *Acta Mater* 53 (2005) 3987–3999, <https://doi.org/10.1016/j.actamat.2005.05.003>.
- [45] R. Gharehbaghi, E.T. Akinlabi, O.S. Fatoba, Experimental investigation of laser metal deposited icosahedral Al–Cu–Fe coatings on grade five titanium alloy, in: *2018 IEEE 9th International Conference on Mechanical and Intelligent Manufacturing Technologies (ICMIMT)*, IEEE, 2018, pp. 31–36.
- [46] A. Saboori, S. Biamino, M. Lombardi, S. Tusacciu, M. Busatto, M. Lai, P. Fino, How the nozzle position affects the geometry of the melt pool in directed energy deposition process, *Powder Metall* 62 (2019) 213–217, <https://doi.org/10.1080/00325899.2019.1627490>.
- [47] J.M. Wilson, C. Piya, Y.C. Shin, F. Zhao, K. Ramani, Remanufacturing of turbine blades by laser direct deposition with its energy and environmental impact analysis, *J. Clean. Prod.* 80 (2014) 170–178, <https://doi.org/10.1016/j.jclepro.2014.05.084>.
- [48] D. Boisselier, S. Sankaré, Influence of powder characteristics in laser direct metal deposition of SS316L for metallic parts manufacturing, *Phys. Procedia* 39 (2012) 455–463, <https://doi.org/10.1016/j.phpro.2012.10.061>.
- [49] D.S. Shim, G.Y. Baek, J.S. Seo, G.Y. Shin, K.P. Kim, K.Y. Lee, Effect of layer thickness setting on deposition characteristics in direct energy deposition (DED) process, *Opt. Laser Technol.* 86 (2016) 69–78, <https://doi.org/10.1016/j.optlastec.2016.07.001>.
- [50] M. Rombouts, G. Maes, M. Mertens, W. Hendrix, Laser metal deposition of Inconel 625: Microstructure and mechanical properties, *J. Laser Appl.* 24 (2012), 052007, <https://doi.org/10.2351/1.4757717>.
- [51] I. Mathoho, E.T. Akinlabi, N. Arthur, M. Tlotleng, Impact of DED process parameters on the metallurgical characteristics of 17-4 PH SS deposited using DED, *CIRP J. Manuf. Sci. Technol.* 31 (2020) 450–458, <https://doi.org/10.1016/j.cirpj.2020.07.007>.
- [52] B.E. Carroll, R.A. Otis, J.P. Borgonia, J. Suh, R.P. Dillon, A.A. Shapiro, D.C. Hofmann, Z.K. Liu, A.M. Beese, Functionally graded material of 304L stainless steel and Inconel 625 fabricated by directed energy deposition: Characterization and thermodynamic modeling, *Acta Mater* 108 (2016) 46–54, <https://doi.org/10.1016/j.actamat.2016.02.019>.
- [53] K.S.B. Ribeiro, F.E. Mariani, R.T. Coelho, A study of different deposition strategies in direct energy deposition (DED) processes, *Procedia Manuf* 48 (2020) 663–670, <https://doi.org/10.1016/j.promfg.2020.05.158>.

- [54] S. Wolff, T. Lee, E. Faierson, K. Ehmann, J. Cao, Anisotropic properties of directed energy deposition (DED)-processed Ti-6Al-4V, *J. Manuf. Process.* 24 (2016) 397–405, <https://doi.org/10.1016/j.jmapro.2016.06.020>.
- [55] Y. Kakinuma, M. Mori, Y. Oda, T. Mori, M. Kashihara, A. Hansel, M. Fujishima, Influence of metal powder characteristics on product quality with directed energy deposition of Inconel 625, *CIRP Ann* 65 (2016) 209–212, <https://doi.org/10.1016/j.cirp.2016.04.058>.
- [56] J.S. Kim, B.J. Kang, S.W. Lee, An experimental study on microstructural characteristics and mechanical properties of stainless-steel 316L parts using directed energy deposition (DED) process, *J. Mech. Sci. Technol.* 33 (2019) 5731–5737, <https://doi.org/10.1007/s12206-019-1116-1>.
- [57] P.A. Kobryn, E.H. Moore, S.L. Semiatin, The effect of laser power and traverse speed on microstructure, porosity, and build height in laser-deposited Ti-6Al-4V, *Scr. Mater.* 43 (2000) 299–305, [https://doi.org/10.1016/S1359-6462\(00\)00408-5](https://doi.org/10.1016/S1359-6462(00)00408-5).
- [58] J. Näsström, J. Frostevarg, A.F.H. Kaplan, Multipass laser hot-wire welding: Morphology and process robustness, *J. Laser Appl.* 29 (2017), 022014, <https://doi.org/10.2351/1.4983758>.
- [59] E. Karadeniz, U. Ozsarac, C. Yildiz, The effect of process parameters on penetration in gas metal arc welding processes, *Mater. Des.* 28 (2007) 649–656, <https://doi.org/10.1016/j.matdes.2005.07.014>.
- [60] X. Shi, S. Ma, C. Liu, Q. Wu, J. Lu, Y. Liu, W. Shi, Selective laser melting-wire arc additive manufacturing hybrid fabrication of Ti-6Al-4V alloy: Microstructure and mechanical properties, *Mater. Sci. Eng. A* 684 (2017) 196–204, <https://doi.org/10.1016/j.msea.2016.12.065>.
- [61] W.U.H. Syed, A.J. Pinkerton, L. Li, Combining wire and coaxial powder feeding in laser direct metal deposition for rapid prototyping, *Appl. Surf. Sci.* 252 (2006) 4803–4808, <https://doi.org/10.1016/j.apsusc.2005.08.118>.
- [62] M. Akbari, R. Kovacevic, Joining of elements fabricated by a robotized laser/wire directed energy deposition process by using an autogenous laser welding, *Int. J. Adv. Manuf.* 100 (2019) 2971–2980, <https://doi.org/10.1007/s00170-018-2891-z>.
- [63] S. Zhang, Y. Zhang, M. Gao, F. Wang, Q. Li, X. Zeng, Effects of milling thickness on wire deposition accuracy of hybrid additive/subtractive manufacturing, *Sci. Technol. Weld. Join.* 24 (2019) 375–381, <https://doi.org/10.1080/13621718.2019.1595925>.
- [64] G. Piscopo, E. Atzeni, A. Salmi, L. Iuliano, A. Gatto, G. Marchiandi, A. Balestrucci, Mesoscale modelling of laser powder-based directed energy deposition process, in: *Procedia CIRP*, 2020, pp. 393–398, <https://doi.org/10.1016/j.procir.2020.05.068>.
- [65] D. Choron, S. Naveos, M. Thomas, J. Petit, D. Boisselier, Direct laser additive manufacturing of TiAl intermetallic compound by powder directed energy deposition (DED), *MATEC Web of Conferences* 321 (2020), 03020, <https://doi.org/10.1051/mateconf/202032103020>.
- [66] M. Gharbi, P. Peyre, C. Gorny, M. Carin, S. Morville, P. le Masson, D. Carron, R. Fabbro, Influence of various process conditions on surface finishes induced by the direct metal deposition laser technique on a Ti-6Al-4V alloy, *Journal of Materials Processing Technology* 213 (2013) 791–800, <https://doi.org/10.1016/j.jmatprotec.2012.11.015>.
- [67] P. Pant, D. Chatterjee, S.K. Samanta, T. Nandi, A.K. Lohar, A bottom-up approach to experimentally investigate the deposition of austenitic stainless steel in laser direct metal deposition system, *Journal of the Brazilian Society of Mechanical Sciences and Engineering* 42 (2020) 88, <https://doi.org/10.1007/s40430-019-2166-0>.
- [68] G. Zhu, D. Li, A. Zhang, G. Pi, Y. Tang, The influence of laser and powder defocusing characteristics on the surface quality in laser direct metal deposition, *Optics and Laser Technology* 44 (2012) 349–356, <https://doi.org/10.1016/j.optlastec.2011.07.013>.
- [69] D. Boisselier, S. Sankaré, T. Engel, Improvement of the laser direct metal deposition process in 5-axis configuration, *Phys. Procedia* 56 (2014) 239–249, <https://doi.org/10.1016/j.phpro.2014.08.168>.
- [70] M.N. Ahsan, A.J. Pinkerton, An analytical–numerical model of laser direct metal deposition track and microstructure formation, *Model. Simul. Mat. Sci. Eng.* 19 (2011), 055003, <https://doi.org/10.1088/0965-0393/19/5/055003>.
- [71] S.Y. Wen, Y.C. Shin, J.Y. Murthy, P.E. Sojka, Modeling of coaxial powder flow for the laser direct deposition process, *Int. J. Heat Mass Transf.* 52 (2009) 5867–5877, <https://doi.org/10.1016/j.ijheatmasstransfer.2009.07.018>.
- [72] M. Moradi, A. Ashoori, A. Hasani, Additive manufacturing of Stellite 6 superalloy by direct laser metal deposition – part 1: Effects of laser power and focal plane position, *Opt. Laser Technol.* 131 (2020) 106328, <https://doi.org/10.1016/j.optlastec.2020.106328>.
- [73] T. DebRoy, T. Mukherjee, J.O. Milewski, J.W. Elmer, B. Ribic, J.J. Blecher, W. Zhang, Scientific, technological and economic issues in metal printing and their solutions, *Nat. Mater.* 18 (2019) 1026–1032, <https://doi.org/10.1038/s41563-019-0408-2>.
- [74] J. Inzana, R. Trombetta, E. Schwarz, S. Kates, H. Awad, 3D printed bioceramics for dual antibiotic delivery to treat implant-associated bone infection, *Eur. Cells Mater.* 30 (2015) 232–247, <https://doi.org/10.22203/eCM.v030a16>.
- [75] M. Khanzadeh, S. Chowdhury, M. Marufuzzaman, M.A. Tschopp, L. Bian, Porosity prediction: supervised-learning of thermal history for direct laser deposition, *J. Manuf. Syst.* 47 (2018) 69–82, <https://doi.org/10.1016/j.jmsy.2018.04.001>.
- [76] Y. Huang, M. Ansari, H. Asgari, M.H. Farshidianfar, D. Sarker, M.B. Khamesee, E. Toyserkani, Rapid prediction of real-time thermal characteristics, solidification parameters and microstructure in laser directed energy deposition (powder-fed additive manufacturing), *J. Mater. Process. Technol.* 274 (2019) 116286, <https://doi.org/10.1016/j.jmatprotec.2019.116286>.
- [77] A. Bagheri, M.J. Mahtabi, N. Shamsaei, Fatigue behavior and cyclic deformation of additive manufactured NiTi, *J. Mater. Process. Technol.* 252 (2018) 440–453, <https://doi.org/10.1016/j.jmatprotec.2017.10.006>.
- [78] M. Megahed, H.W. Mindt, N. N'Dri, H. Duan, O. Desmaison, Metal additive-manufacturing process and residual stress modeling, *Integr. Mater. Manuf. Innov.* 5 (2016) 61–93, <https://doi.org/10.1186/s40192-016-0047-2>.
- [79] W.J. Sames, F.A. List, S. Pannala, R.R. Dehoff, S.S. Babu, The metallurgy and processing science of metal additive manufacturing, *Int. Mater. Rev.* 61 (2016) 315–360, <https://doi.org/10.1080/09506608.2015.1116649>.
- [80] C. Xia, Z. Pan, J. Polden, H. Li, Y. Xu, S. Chen, Y. Zhang, A review on wire arc additive manufacturing: Monitoring, control and a framework of automated system, *J. Manuf. Syst.* 57 (2020) 31–45, <https://doi.org/10.1016/j.jmsy.2020.08.008>.
- [81] Y. Yang, Y. Gong, S. Qu, G. Yin, C. Liang, P. Li, Additive and subtractive hybrid manufacturing (ASHM) of 316L stainless steel: Single-track specimens, microstructure, and mechanical properties, *JOM* 73 (2021) 759–769, <https://doi.org/10.1007/s11837-020-04216-2>.
- [82] Y.A. Song, S. Park, Experimental investigations into rapid prototyping of composites by novel hybrid deposition process, *J. Mater. Process. Technol.* 171 (2006) 35–40, <https://doi.org/10.1016/j.jmatprotec.2005.06.062>.
- [83] J. Hur, K. Lee, Zhu-hu, J. Kim, Hybrid rapid prototyping system using machining and deposition, *Comput. Aided Des.* 34 (2002) 741–754, [https://doi.org/10.1016/S0010-4485\(01\)00203-2](https://doi.org/10.1016/S0010-4485(01)00203-2).
- [84] M. Merklein, R. Schulte, T. Papke, An innovative process combination of additive manufacturing and sheet bulk metal forming for manufacturing a functional hybrid part, *J. Mater. Process. Technol.* 291 (2021) 117032, <https://doi.org/10.1016/j.jmatprotec.2020.117032>.
- [85] P. Kunwar, Z. Xiong, S.T. Mcloughlin, P. Soman, Oxygen-permeable films for continuous additive, subtractive, and hybrid additive/subtractive manufacturing, *3D Print. Addit. Manuf.* 7 (2020) 216–221, <https://doi.org/10.1089/3dp.2019.0166>.
- [86] S.Y. Liang, Y. Feng, J. Ning, Predictive manufacturing: subtractive and additive, *IOP Conf. Ser.: Mater. Sci. Eng.* 842 (2020), 012024, <https://doi.org/10.1088/1757-899X/842/1/012024>.
- [87] F. Liravi, E. Toyserkani, A hybrid additive manufacturing method for the fabrication of silicone bio-structures: 3D printing optimization and surface characterization, *Mater. Des.* 138 (2018) 46–61, <https://doi.org/10.1016/j.matdes.2017.10.051>.
- [88] G. Djogo, J. Li, S. Ho, M. Haque, E. Ertorer, J. Liu, X. Song, J. Suo, P.R. Herman, Femtosecond laser additive and subtractive micro-processing: Enabling a high-channel-density silica interposer for multicore fibre to silicon-photonics packaging, *Int. J. Ext. Manuf.* 1 (2019), 045002, <https://doi.org/10.1088/2631-7990/ab4d51>.
- [89] R.J. Friel, R.A. Harris, Ultrasonic additive manufacturing – A hybrid production process for novel functional products, *Procedia CIRP* 6 (2013) 35–40, <https://doi.org/10.1016/j.procir.2013.03.004>.
- [90] J. Butt, Y. Hewavidana, V. Mohaghegh, S. Sadeghi-Esfahani, H. Shirvani, Hybrid manufacturing and experimental testing of glass fiber enhanced thermoplastic composites, *J. Manuf. Mater. Process.* 3 (2019) 96, <https://doi.org/10.3390/jmmp3040096>.
- [91] (Peter) Liu, N. Gershenfeld, Performance comparison of subtractive and additive machine tools for meso-micro machining, *J. Manuf. Mater. Process.* 4 (2020) 19, <https://doi.org/10.3390/jmmp4010019>.
- [92] P. Mogno, M. Rivette, L. Jégou, T. Lesprier, A first approach to choose between HSM, EDM and DMLS processes in hybrid rapid tooling, *Rapid Prototyp. J.* 13 (2007) 7–16, <https://doi.org/10.1108/13552540710719163>.
- [93] Z. Zhu, V. Dhokia, S.T. Newman, The development of a novel process planning algorithm for an unconstrained hybrid manufacturing process, *J. Manuf. Process.* 15 (2013) 404–413, <https://doi.org/10.1016/j.jmapro.2013.06.006>.
- [94] L. Li, A. Haghghi, Y. Yang, Theoretical modelling and prediction of surface roughness for hybrid additive–subtractive manufacturing processes, *IIEE Trans* 51 (2019) 124–135, <https://doi.org/10.1080/24725854.2018.1458268>.
- [95] J.B. Jones, *The synergies of hybridizing CNC and additive manufacturing*, *Soc. of Manuf. Eng.*, 2014.
- [96] S. Akula, K.P. Karunakaran, Hybrid adaptive layer manufacturing: An intelligent art of direct metal rapid tooling process, *Robot. Comput. Integr. Manuf.* 22 (2006) 113–123, <https://doi.org/10.1016/j.rcim.2005.02.006>.
- [97] C. Hodonou, O. Kerbrat, M. Balazinski, M. Brochu, Process selection charts based on economy and environment: Subtractive or additive manufacturing to produce structural components of aircraft, *Int. J. Interact. Des. Manuf.* 14 (2020) 861–873, <https://doi.org/10.1007/s12008-020-00663-y>.
- [98] K. Salonitis, L. D'Alvise, B. Schoinochoritis, D. Chantzis, Additive manufacturing and post-processing simulation: Laser cladding followed by high speed machining, *Int. J. Adv. Manuf.* 85 (2016) 2401–2411, <https://doi.org/10.1007/s00170-015-7989-y>.
- [99] J.M. Flynn, A. Shokrani, S.T. Newman, V. Dhokia, Hybrid additive and subtractive machine tools – Research and industrial developments, *Int. J. Mach. Tools Manuf.* 101 (2016) 79–101, <https://doi.org/10.1016/j.ijmactools.2015.11.007>.
- [100] B. Nau, A. Roderburg, F. Klocke, Ramp-up of hybrid manufacturing technologies, *CIRP J. Manuf. Sci. Technol.* 4 (2011) 313–316, <https://doi.org/10.1016/j.cirpj.2011.04.003>.

- [101] M. Lutter-Günther, S. Wagner, C. Seidel, G. Reinhart, Economic and ecological evaluation of hybrid additive manufacturing technologies based on the combination of laser metal deposition and CNC machining, *Appl. Mech. Mater.* 805 (2015) 213–222, <https://doi.org/10.4028/www.scientific.net/AMM.805.213>.
- [102] K. Boivie, S. Dolinsek, D. Homar, Hybrid manufacturing; integration of additive technologies for competitive production of complex tools and products, in: 15th International Research/Expert Conference "Trends in the Development of Machinery and Associated Technology", 2011, p. 35.
- [103] D. Strong, M. Kay, B. Conner, T. Wakefield, G. Manogharan, Hybrid manufacturing – Integrating traditional manufacturers with additive manufacturing (AM) supply chain, *Addit. Manuf.* 21 (2018) 159–173, <https://doi.org/10.1016/j.addma.2018.03.010>.
- [104] A. Nassehi, S. Newman, V. Dhokia, Z. Zhu, R.I. Asrai, Using formal methods to model hybrid manufacturing processes, in: *Enabling Manufacturing Competitiveness and Economic Sustainability*, Springer Berlin Heidelberg, Berlin, Heidelberg, 2012, pp. 52–56, https://doi.org/10.1007/978-3-642-23860-4_8.
- [105] M. Soshi, J. Ring, C. Young, Y. Oda, M. Mori, Innovative grid molding and cooling using an additive and subtractive hybrid CNC machine tool, *CIRP Ann* 66 (2017) 401–404, <https://doi.org/10.1016/j.cirp.2017.04.093>.
- [106] V. Benoist, L. Arnaud, M. Baili, A new method of design for additive manufacturing including machining constraints, *Int. J. Adv. Manuf. Technol.* 111 (2020) 25–36, <https://doi.org/10.1007/s00170-020-06059-2>.
- [107] O. Kerbrat, P. Mogno, J.Y. Hascoët, A new DFM approach to combine machining and additive manufacturing, *Comput. Ind.* 62 (2011) 684–692, <https://doi.org/10.1016/j.compind.2011.04.003>.
- [108] A.E. Patterson, J.T. Allison, Manufacturability constraint formulation for design under hybrid additive-subtractive manufacturing, in: 23rd Design for Manufacturing and the Life Cycle Conference; 12th International Conference on Micro- and Nanosystems, American Society of Mechanical Engineers, 2018, <https://doi.org/10.1115/DETC2018-85637>.
- [109] Y.S. Han, B. Xu, L. Zhao, Y.M. Xie, Topology optimization of continuum structures under hybrid additive-subtractive manufacturing constraints, *Struct. Multidiscipl. Optim.* 60 (2019) 2571–2595, <https://doi.org/10.1007/s00158-019-02334-3>.
- [110] J. Liu, A.C. To, Topology optimization for hybrid additive-subtractive manufacturing, *Struct. Multidiscipl. Optim.* 55 (2017) 1281–1299, <https://doi.org/10.1007/s00158-016-1565-4>.
- [111] J. Liu, Y. Zheng, Y. Ma, A. Qureshi, R. Ahmad, A topology optimization method for hybrid subtractive-additive remanufacturing, *Int. J. Precis. Eng. Manuf. - Green Technol.* 7 (2020) 939–953, <https://doi.org/10.1007/s40684-019-00075-8>.
- [112] Y. Yang, Y. Gong, C. Li, X. Wen, J. Sun, Mechanical performance of 316 L stainless steel by hybrid directed energy deposition and thermal milling process, *J. Mater. Process. Technol.* 291 (2021) 117023, <https://doi.org/10.1016/j.jmatprotec.2020.117023>.
- [113] J.L. Dávila, P.I. Neto, P.Y. Noritomi, R.T. Coelho, J.V.L. da Silva, Hybrid manufacturing: A review of the synergy between directed energy deposition and subtractive processes, *Int. J. Adv. Manuf. Technol.* 110 (2020) 3377–3390, <https://doi.org/10.1007/s00170-020-06062-7>.
- [114] M. Kerschbaumer, G. Ernst, Hybrid manufacturing process for rapid high performance tooling combining high speed milling and laser cladding, in: *International Congress on Applications of Lasers & Electro-Optics*, Laser Institute of America, 2004, p. 1710, <https://doi.org/10.2351/1.5060234>.
- [115] F.W. Liou, J. Choi, R.G. Landers, V. Janardhan, S.N. Balakrishnan, S. Agarwal, Research and development of a hybrid rapid manufacturing process f, in: *Proceedings of the Solid Freeform Fabrication Symposium*, 2001, <https://doi.org/10.26153/tsw/3246>.
- [116] T. Yamazaki, Development of a hybrid multi-tasking machine tool: integration of additive manufacturing technology with CNC machining, *Procedia CIRP* 42 (2016) 81–86, <https://doi.org/10.1016/j.procir.2016.02.193>.
- [117] I. Gibson, D. Rosen, B. Stucker, M. Khorasani, Hybrid additive manufacturing, in: I. Gibson, D. Rosen, B. Stucker, M. Khorasani (Eds.), *Additive Manufacturing Technologies*, Springer International Publishing, Cham, 2021, pp. 347–366, https://doi.org/10.1007/978-3-030-56127-7_12.
- [118] S. Linnenbrink, M. Alkhayati, N. Pirch, A. Gasser, H. Schleifenbaum, DED for repair and manufacture of turbomachinery components, in: *3D Printing for Energy Applications*, Wiley, 2021, pp. 307–326, <https://doi.org/10.1002/9781119560807.ch12>.
- [119] E.M. Sefene, Y.M. Hailu, A.A. Tsegaw, Metal hybrid additive manufacturing: State-of-the-art, *Prog. Addit. Manuf.* (2022), <https://doi.org/10.1007/s40964-022-00262-1>.
- [120] W. Zhang, M. Soshi, K. Yamazaki, Development of an additive and subtractive hybrid manufacturing process planning strategy of planar surface for productivity and geometric accuracy, *Int. J. Adv. Manuf. Technol.* 109 (2020) 1479–1491, <https://doi.org/10.1007/s00170-020-05733-9>.
- [121] Y. Xie, J. Tong, Y. Fu, Z. Sheng, Machining scheme of aviation bearing bracket based on additive and subtractive hybrid manufacturing, *J. Mech. Sci. Technol.* 34 (2020) 3775–3790, <https://doi.org/10.1007/s12206-020-0829-5>.
- [122] N. Chen, M. Frank, Process planning for hybrid additive and subtractive manufacturing to integrate machining and directed energy deposition, *Procedia Manuf* 34 (2019) 205–213, <https://doi.org/10.1016/j.promfg.2019.06.140>.
- [123] J.C. Heigel, T.Q. Phan, J.C. Fox, T.H. Gnaupel-Herold, Experimental investigation of residual stress and its impact on machining in hybrid additive/subtractive manufacturing, *Procedia Manuf* 26 (2018) 929–940, <https://doi.org/10.1016/j.promfg.2018.07.120>.
- [124] F. Liou, K. Slattery, M. Kinsella, J. Newkirk, H. Chou, R. Landers, Applications of a hybrid manufacturing process for fabrication of metallic structures, *Rapid Prototyp. J.* 13 (2007) 236–244, <https://doi.org/10.1108/13552540710776188>.
- [125] L. Ren, A.P. Padathu, J. Ruan, T. Sparks, F.W. Liou, Three dimensional die repair using a hybrid manufacturing system, in: *17th Solid Freeform Fabrication Symposium, SFF*, 2006, 2006.
- [126] K.P. Karunakaran, V. Pushpa, S.B. Akula, S. Suryakumar, Techno-economic analysis of hybrid layered manufacturing, *Int. J. Intell. Syst. Technol. Appl.* 4 (2008) 161, <https://doi.org/10.1504/IJISTA.2008.016364>.
- [127] K.P. Karunakaran, S. Suryakumar, V. Pushpa, S. Akula, Low cost integration of additive and subtractive processes for hybrid layered manufacturing, *Robot. Comput. Integr. Manuf.* 26 (2010) 490–499, <https://doi.org/10.1016/j.rcim.2010.03.008>.
- [128] A. Sreenathbabu, K.P. Karunakaran, C. Amarnath, Statistical process design for hybrid adaptive layer manufacturing, *Rapid Prototyp. J.* 11 (2005) 235–248, <https://doi.org/10.1108/13552540510612929>.
- [129] Y. Yang, Y. Gong, S. Qu, B. Xin, Y. Xu, Y. Qi, Additive/subtractive hybrid manufacturing of 316L stainless steel powder: Densification, microhardness and residual stress, *J. Mech. Sci. Technol.* 33 (2019) 5797–5807, <https://doi.org/10.1007/s12206-019-1126-z>.
- [130] O. Oyelola, P. Crawforth, R. M'Saoubi, A.T. Clare, On the machinability of directed energy deposited Ti6Al4V, *Addit. Manuf.* 19 (2018) 39–50, <https://doi.org/10.1016/j.addma.2017.11.005>.
- [131] O. Oyelola, P. Crawforth, R. M'Saoubi, A.T. Clare, Machining of additively manufactured parts: Implications for surface integrity, *Procedia CIRP* 45 (2016) 119–122, <https://doi.org/10.1016/j.procir.2016.02.066>.
- [132] A. Seidel, A. Straubel, T. Finaske, T. Maiwald, S. Polenz, M. Albert, J. Näsström, A. Riecke, M. Riede, E. Lopez, F. Brueckner, E. Beyer, C. Leyens, Added value by hybrid additive manufacturing and advanced manufacturing approaches, *J. Laser Appl.* 30 (2018), 032301, <https://doi.org/10.2351/1.5040632>.
- [133] V.v. Popov, A. Fleisher, Hybrid additive manufacturing of steels and alloys, *Manuf. Rev.* 7 (2020) 6, <https://doi.org/10.1051/mfreview/20200005>.
- [134] A. Al-Ahmari, M. Ashfaq, A. Alfaifi, B. Abdo, A. Alomar, A. Dawud, Predicting surface quality of γ -TiAl produced by additive manufacturing process using response surface method, *J. Mech. Sci. Technol.* 30 (2016) 345–352, <https://doi.org/10.1007/s12206-015-1239-y>.
- [135] N. Chernovol, A. Sharma, T. Tjahjowidodo, B. Lauwers, P. van Rymentant, Machinability of wire and arc additive manufactured components, *CIRP J. Manuf. Sci. Technol.* 35 (2021) 379–389, <https://doi.org/10.1016/j.cirpj.2021.06.022>.
- [136] J.G. Lopes, C.M. Machado, V.R. Duarte, T.A. Rodrigues, T.G. Santos, J.P. Oliveira, Effect of milling parameters on HSLA steel parts produced by wire and arc additive manufacturing (WAAM), *J. Manuf. Process.* 59 (2020) 739–749, <https://doi.org/10.1016/j.jmapro.2020.10.007>.
- [137] A. Dass, A. Moridi, State of the art in directed energy deposition: From additive manufacturing to materials design, *Coatings* 9 (2019) 418, <https://doi.org/10.3390/coatings9070418>.
- [138] A.M. Beese, B.E. Carroll, Review of mechanical properties of Ti–6Al–4V made by laser-based additive manufacturing using powder feedstock, *JOM* 68 (2016) 724–734, <https://doi.org/10.1007/s11837-015-1759-z>.
- [139] B. Dutta, F.H. (Sam, Froes, The additive manufacturing (AM) of titanium alloys, *Met. Powder Rep.* 72 (2017) 96–106, <https://doi.org/10.1016/j.mprp.2016.12.062>.
- [140] B. Baufeld, O. van der Biest, Mechanical properties of Ti–6Al–4V specimens produced by shaped metal deposition, *Sci. Technol. Adv. Mater.* 10 (2009), 015008, <https://doi.org/10.1088/1468-6996/10/1/015008>.
- [141] B.A. Szost, S. Terzi, F. Martina, D. Boisselier, A. Prytuliak, T. Pirling, M. Hofmann, D.J. Jarvis, A comparative study of additive manufacturing techniques: Residual stress and microstructural analysis of CLAD and WAAM printed Ti–6Al–4V components, *Mater. Des.* 89 (2016) 559–567, <https://doi.org/10.1016/j.matdes.2015.09.115>.
- [142] C. Dharmendra, S. Shakerin, G.D.J. Ram, M. Mohammadi, Wire-arc additive manufacturing of nickel aluminum bronze/stainless steel hybrid parts – Interfacial characterization, prospects, and problems, *Materialia* (Oxf). 13 (2020) 100834, <https://doi.org/10.1016/j.mta.2020.100834>.
- [143] T. Feldhausen, N. Raghavan, K. Saleeb, L. Love, T. Kurfess, Mechanical properties and microstructure of 316L stainless steel produced by hybrid manufacturing, *J. Mater. Process. Technol.* 290 (2021) 116970, <https://doi.org/10.1016/j.jmatprotec.2020.116970>.
- [144] B. Baufeld, O. van der Biest, R. Gault, Additive manufacturing of Ti–6Al–4V components by shaped metal deposition: Mechanical properties, *Mater. Des.* 31 (2010) S106–S111, <https://doi.org/10.1016/j.matdes.2009.11.032>.
- [145] F.J. Xu, Y.H. Lv, B.S. Xu, Y.X. Liu, F.Y. Shu, P. He, Effect of deposition strategy on the microstructure and mechanical properties of Inconel 625 superalloy fabricated by pulsed plasma arc deposition, *Mater. Des.* 45 (2013) 446–455, <https://doi.org/10.1016/j.matdes.2012.07.013>.
- [146] B. Baufeld, E. Brandl, O. van der Biest, Wire based additive layer manufacturing: Comparison of microstructure and mechanical properties of Ti–6Al–4V components fabricated by laser-beam deposition and shaped metal deposition, *J. Mater. Process. Technol.* 211 (2011) 1146–1158, <https://doi.org/10.1016/j.jmatprotec.2011.01.018>.
- [147] F. Wang, S. Williams, P. Colegrove, A.A. Antony, Microstructure and mechanical properties of wire and arc additive manufactured Ti–6Al–4V, *Metall. Mater. Trans. A* 44 (2013) 968–977, <https://doi.org/10.1007/s11661-012-1444-6>.

- [148] E. Brandl, B. Baufeld, C. Leyens, R. Gault, Additive manufactured Ti–6Al–4V using welding wire: Comparison of laser and arc beam deposition and evaluation with respect to aerospace material specifications, *Phys. Procedia*. 5 (2010) 595–606, <https://doi.org/10.1016/j.phpro.2010.08.087>.
- [149] Y. Liu, W. Wang, J. Xie, S. Sun, L. Wang, Y. Qian, Y. Meng, Y. Wei, Microstructure and mechanical properties of aluminum 5083 weldments by gas tungsten arc and gas metal arc welding, *Mater. Sci. Eng. A*. 549 (2012) 7–13, <https://doi.org/10.1016/j.msea.2012.03.108>.
- [150] C. Wang, T.G. Liu, P. Zhu, Y.H. Lu, T. Shoji, Study on microstructure and tensile properties of 316L stainless steel fabricated by CMT wire and arc additive manufacturing, *Mater. Sci. Eng. A*. 796 (2020) 140006, <https://doi.org/10.1016/j.msea.2020.140006>.
- [151] B. Baufeld, Mechanical properties of Inconel 718 parts manufactured by shaped metal deposition (SMD), *J. Mater. Eng. Perform.* 21 (2012) 1416–1421, <https://doi.org/10.1007/s11665-011-0009-y>.
- [152] V.T. Le, D.S. Mai, T.K. Doan, H. Paris, Wire and arc additive manufacturing of 308L stainless steel components: Optimization of processing parameters and material properties, *Eng. Sci. Technol. an Int. J.* 24 (2021) 1015–1026, <https://doi.org/10.1016/j.jestch.2021.01.009>.
- [153] D. Kumar, S. Jhavar, A. Arya, K.G. Prashanth, S. Suwas, Mechanisms controlling fracture toughness of additively manufactured stainless steel 316L, *Int. J. Fract.* (2021), <https://doi.org/10.1007/s10704-021-00574-3>.
- [154] J.J. Lin, Y.H. Lv, Y.X. Liu, B.S. Xu, Z. Sun, Z.G. Li, Y.X. Wu, Microstructural evolution and mechanical properties of Ti–6Al–4V wall deposited by pulsed plasma arc additive manufacturing, *Mater. Des.* 102 (2016) 30–40, <https://doi.org/10.1016/j.matdes.2016.04.018>.
- [155] J. Lin, Y. Lv, Y. Liu, Z. Sun, K. Wang, Z. Li, Y. Wu, B. Xu, Microstructural evolution and mechanical property of Ti–6Al–4V wall deposited by continuous plasma arc additive manufacturing without post heat treatment, *J. Mech. Behav. Biomed. Mater.* 69 (2017) 19–29, <https://doi.org/10.1016/j.jmbbm.2016.12.015>.
- [156] F. Xu, Y. Lv, Y. Liu, F. Shu, P. He, B. Xu, Microstructural evolution and mechanical properties of Inconel 625 alloy during pulsed plasma arc deposition process, *J. Mater. Sci. Technol.* 29 (2013) 480–488, <https://doi.org/10.1016/j.jmst.2013.02.010>.
- [157] C. Qiu, G.A. Ravi, C. Dance, A. Ranson, S. Dilworth, M.M. Attallah, Fabrication of large Ti–6Al–4V structures by direct laser deposition, *J. Alloys Compd.* 629 (2015) 351–361, <https://doi.org/10.1016/j.jallcom.2014.12.234>.
- [158] E. Amsterdam, G.A. Kool, High cycle fatigue of laser beam deposited Ti–6Al–4V and Inconel 718, in: *ICAF 2009, Bridging the Gap between Theory and Operational Practice*, Springer Netherlands, Dordrecht, 2009, pp. 1261–1274.
- [159] J. Alcisto, A. Enriquez, H. Garcia, S. Hinkson, T. Steelman, E. Silverman, P. Valdovino, H. Gigerenzer, J. Foyos, J. Ogren, J. Dorey, K. Karg, T. McDonald, O.S. Es-Said, Tensile properties and microstructures of laser-formed Ti–6Al–4V, *J. Mater. Eng. Perform.* 20 (2011) 203–212, <https://doi.org/10.1007/s11665-010-9670-9>.
- [160] L.Y. Qin, J.H. Men, L.S. Zhang, S. Zhao, C.F. Li, G. Yang, W. Wang, Microstructure homogenizations of Ti–6Al–4V alloy manufactured by hybrid selective laser melting and laser deposition manufacturing, *Mater. Sci. Eng. A*. 759 (2019) 404–414, <https://doi.org/10.1016/j.msea.2019.05.049>.
- [161] T. Gu, B. Chen, C. Tan, J. Feng, Microstructure evolution and mechanical properties of laser additive manufacturing of high strength Al–Cu–Mg alloy, *Opt. Laser Technol.* 112 (2019) 140–150, <https://doi.org/10.1016/j.optlastec.2018.11.008>.
- [162] A. Saboori, G. Piscopo, M. Lai, A. Salmi, S. Biamino, An investigation on the effect of deposition pattern on the microstructure, mechanical properties and residual stress of 316L produced by directed energy deposition, *Mater. Sci. Eng. A*. 780 (2020) 139179, <https://doi.org/10.1016/j.msea.2020.139179>.
- [163] E. Azinpour, R. Darabi, J. Cesar de Sa, A. Santos, J. Hodek, J. Dzugan, Fracture analysis in directed energy deposition (DED) manufactured 316L stainless steel using a phase-field approach, *Finite Elem. Anal. Des.* 177 (2020) 103417, <https://doi.org/10.1016/j.finel.2020.103417>.
- [164] T.R. Smith, J.D. Sugar, C. San Marchi, J.M. Schoenung, Orientation effects on fatigue behavior of additively manufactured stainless steel, in: *Materials and Fabrication*, American Society of Mechanical Engineers, 2017, <https://doi.org/10.1115/PVP2017-65948>.
- [165] P. Guo, B. Zou, C. Huang, H. Gao, Study on microstructure, mechanical properties and machinability of efficiently additive manufactured AISI 316L stainless steel by high-power direct laser deposition, *J. Mater. Process. Technol.* 240 (2017) 12–22, <https://doi.org/10.1016/j.jmatprotec.2016.09.005>.
- [166] K. Zhang, S. Wang, W. Liu, X. Shang, Characterization of stainless steel parts by laser metal deposition shaping, *Mater. Des.* 55 (2014) 104–119, <https://doi.org/10.1016/j.matdes.2013.09.006>.
- [167] A. Hansel, M. Mori, M. Fujishima, Y. Oda, G. Hyatt, E. Lavernia, J.P. Delplanque, Study on consistently optimum deposition conditions of typical metal material using additive/subtractive hybrid machine tool, *Procedia CIRP* 46 (2016) 579–582, <https://doi.org/10.1016/j.procir.2016.04.113>.
- [168] Y. Gong, Y. Yang, S. Qu, P. Li, C. Liang, H. Zhang, Laser energy density dependence of performance in additive/subtractive hybrid manufacturing of 316L stainless steel, *Int. J. Adv. Manuf. Technol.* 105 (2019) 1585–1596, <https://doi.org/10.1007/s00170-019-04372-z>.
- [169] W.S. Woo, E.J. Kim, H.I. Jeong, C.M. Lee, Laser-assisted machining of Ti–6Al–4V fabricated by DED additive manufacturing, *Int. J. Precis. Eng. Manuf. Green Technol.* 7 (2020) 559–572, <https://doi.org/10.1007/s40684-020-00221-7>.
- [170] B.K. Dey, B. Sarkar, H. Seok, Cost-effective smart automation policy for a hybrid manufacturing-remanufacturing, *Comput. Ind. Eng.* 162 (2021) 107758, <https://doi.org/10.1016/j.cie.2021.107758>.
- [171] Ch Achillas, D. Aidonis, E. Iakovou, M. Thymianidis, D. Tzetzis, A methodological framework for the inclusion of modern additive manufacturing into the production portfolio of a focused factory, *J. Manuf. Syst.* 37 (2015) 328–339, <https://doi.org/10.1016/j.jmsy.2014.07.014>.
- [172] A. Wippermann, T.G. Gutowski, B. Denkena, M.A. Dittrich, Y. Wessargues, Electrical energy and material efficiency analysis of machining, additive and hybrid manufacturing, *J. Clean. Prod.* 251 (2020) 119731, <https://doi.org/10.1016/j.jclepro.2019.119731>.
- [173] W. Liu, K. Deng, H. Wei, P. Zhao, J. Li, Y. Zhang, A decision-making model for comparing the energy demand of additive-subtractive hybrid manufacturing and conventional subtractive manufacturing based on life cycle method, *J. Clean. Prod.* 311 (2021) 127795, <https://doi.org/10.1016/j.jclepro.2021.127795>.
- [174] G. Manogharan, R.A. Wysk, O.L.A. Harrysson, Additive manufacturing-integrated hybrid manufacturing and subtractive processes: Economic model and analysis, *Int. J. Comput. Integr. Manuf.* 29 (2016) 473–488, <https://doi.org/10.1080/0951192X.2015.1067920>.
- [175] G. Manogharan, R. Wysk, O. Harrysson, R. Aman, AIMS – A metal additive-hybrid manufacturing system: System architecture and attributes, *Procedia Manuf* 1 (2015) 273–286, <https://doi.org/10.1016/j.promfg.2015.09.021>.
- [176] M. Cortina, J. Arrizubieta, J. Ruiz, E. Ukar, A. Lamikiz, Latest developments in industrial hybrid machine tools that combine additive and subtractive operations, *Materials* 11 (2018) 2583, <https://doi.org/10.3390/ma11122583>.
- [177] T.A. Rodrigues, V.R. Duarte, R.M. Miranda, T.G. Santos, J.P. Oliveira, Ultracold-wire and arc additive manufacturing (UC-WAAM), *J. Mater. Process. Technol.* 296 (2021) 117196, <https://doi.org/10.1016/j.jmatprotec.2021.117196>.
- [178] P.G. Benardos, G.C. Vosniakos, Predicting surface roughness in machining: A review, *Int. J. Mach. Tools Manuf.* 43 (2003) 833–844, [https://doi.org/10.1016/S0890-6955\(03\)00059-2](https://doi.org/10.1016/S0890-6955(03)00059-2).
- [179] A. Coro, L.M. Macareno, J. Aguirrebeitia, L.N. López de Lacalle, A methodology to evaluate the reliability impact of the replacement of welded components by additive manufacturing spare parts, *Metals (Basel)* 9 (2019) 932, <https://doi.org/10.3390/met9090932>.
- [180] M. Salmi, I.F. Ituarte, S. Chekurov, E. Huotilainen, Effect of build orientation in 3D printing production for material extrusion, material jetting, binder jetting, sheet optical lamination, vat photopolymerisation, and powder bed fusion, *Int. J. Collab. Enterp.* 5 (2016) 218, <https://doi.org/10.1504/IJCENT.2016.082334>.
- [181] L.E. Criales, Y.M. Arnsay, B. Lane, S. Moylan, A. Donnez, T. Özel, Laser powder bed fusion of nickel alloy 625: Experimental investigations of effects of process parameters on melt pool size and shape with spatter analysis, *Int. J. Mach. Tools Manuf.* 121 (2017) 22–36, <https://doi.org/10.1016/j.ijmactools.2017.03.004>.
- [182] Z. Fan, B. Li, Meshfree simulations for additive manufacturing process of metals, *Integr. Mater. Manuf. Innov.* 8 (2019) 144–153, <https://doi.org/10.1007/s40192-019-00131-w>.
- [183] M. Carraturo, B. Lane, H. Yeung, S. Kollmannsberger, A. Reali, F. Auricchio, Numerical evaluation of advanced laser control strategies influence on residual stresses for laser powder bed fusion systems, *Integr. Mater. Manuf. Innov.* 9 (2020) 435–445, <https://doi.org/10.1007/s40192-020-00191-3>.
- [184] M. Merklein, D. Junker, A. Schaub, F. Neubauer, Hybrid additive manufacturing technologies – An analysis regarding potentials and applications, *Phys. Procedia* 83 (2016) 549–559, <https://doi.org/10.1016/j.phpro.2016.08.057>.



Mohammadreza Lalegani Dezaki received his MSc degree in Manufacturing Systems Engineering from Universiti Putra Malaysia (UPM). He has published several papers in the field of 3D printing. In 2021, He was awarded a PhD Studentship issued by Nottingham Trent University (NTU). His current research interests involve 3D printing and smart soft actuators for soft robots.



Ahmad Serjouei completed his BSc (Mech. Eng.) at Isfahan University of Technology (IUT), Iran in 2007. He obtained his MEng and PhD from Nanyang Technological University (NTU), Singapore in 2009 and 2014. He is a Chartered Engineer (CEng) and holds Fellow of Higher Education Academy (FHEA) and Postgraduate Certificate in Academic Practice (PGCAP) certificates for teaching. He has been a senior lecturer at Nottingham Trent University (NTU), UK since 2019. His research interests include mechanics of materials, 3D and 4D printing, metal additive manufacturing, smart materials and structures, and soft actuation.



Ali Zolfagharian is among the 2% top cited scientists listed by Stanford University and Elsevier (2020), the Alfred Deakin Medalist for Best Doctoral Thesis (2019), and the Alfred Deakin Postdoctoral Fellowship Awardee (2018). He is co-founder of the 4D Printing Society, co-editor of the Smart Materials in Additive Manufacturing book series published by Elsevier, and a senior lecturer in the School of Engineering at Deakin University, Australia. His 4D Printing and Robotic Materials lab established in Australia in 2018. He has thus far received AUD \$183k research support funds from academic and industrial firms. His recent research outputs in the field of 3D and 4D printing include 69 articles, being editor of 2 journals, 5 books, and special issues.



Mohd Khairol received his PhD in mechanical engineering from University of Sheffield. He is a professor in department of mechanical and manufacturing engineering at Universiti Putra Malaysia (UPM). He has published more than 200 papers in international, national journals and conferences. He is a member of Board of Engineers Malaysia (BEM) and Malaysian Society for Engineering and Technology. His current research interests include, machining, industrial engineering, finite element analysis and optimisation.



Mohammad is an assistant professor in the faculty of civil engineering and geosciences at TU Delft. He has published over 140 scientific papers, 2 book chapters and 3 filed patents. He led the hybrid composites developments in the HiPerDuCT programme (EP/102946X/1, a UK research council grant), and have secured research grants as a principal investigator, led UK research council grants (EP/V009451/1 and EP/R511705/1) and industrial projects related to SHM of composite structures. He has 3 years of industrial experience in research & development (R&D) activities on design, manufacturing, and analysis of engineering materials. He received 2 research excellence awards from the University of Glasgow, was nominated as the best researcher of the year at the University of the West of England's aerospace department.



Dr Mahdi Bodaghi (BSc, MSc, PhD, PGCAP, FHEA, CEng, MIMechE) is an Assistant Professor in the Department of Engineering, School of Science and Technology at Nottingham Trent University. Mahdi heads the 4D Materials & Printing Laboratory (4DMPL) that hosts a broad portfolio of projects focusing on the electro-thermomechanical multi-scale behaviours of smart materials, soft robots, and 3D/4D printing technologies. In the recent twelve years, he has been working towards the advancement of state-of-the-art smart materials and additive manufacturing leading him to co-found the 4D Printing Society in 2021, and to co-edit Smart Materials in Additive Manufacturing book series published by Elsevier in 2022. His research has led to the publication of over 120 scientific papers in leading journals in mechanics, manufacturing and materials science, and the presentation of his work at major international conferences. Mahdi has also served as Chairman and member of Scientific Committees for 10 International Conferences, as Guest Editor for 8 scientific Journals, as Editorial Board Member for 8 Journals, and as Reviewer for over 130 Journals. Mahdi's research awards include the Best Doctoral Thesis Award of 2015, the Best Paper Award in Mechanics and Material Systems presented by the American Society of Mechanical Engineers (ASME) in 2015, and 2021 IJPEM-GT Contribution Award recognized by the Korea Society for Precision Engineering.



Dr. Mahmoud Moradi is currently Assistant Professor at Coventry University in the UK. He has been active in laser materials processing for 17 years. His main scientific contributions have been laser materials processing, non-traditional machining, welding technology, additive manufacturing, and 3D/4D printing. He has published more than 150 papers in international and national journals and conferences and 9 book chapters in the areas of his interests. He was a scientific committee member, keynote speaker, workshop presenter, chairman, and chair of panels for various international conferences. He is an editorial board member and guest editor of several reputable journals. he was featured in the list of "World Ranking of Top 2% Scientists in the World" in the 2020 & 2021 database based on a Stanford University report.